Research Report 163

LABORATORY DETERMINATION OF DYNAMIC MODULI OF FROZEN SOILS AND OF ICE

Chester W. Kaplar

January 1969

DA TASK 1T062112A13001

U.S. ARMY MATERIEL COMMAND
TERRESTRIAL SCIENCES CENTER
COLD REGIONS RESEARCH & ENGINEERING LABORATORY
HANOVER, NEW HAMPSHIRE

THIS DOCUMENT HAS BEEN APPROVED FOR PUBLIC RELEASE AND SALE; ITS DISTRIBUTION IS UNLIMITED.

PREFACE

The investigation reported herein is part of a comprehensive investigation and study of methods for description, classification and determination of the strength properties of frozen soils and ice-soil mixtures conducted by the Arctic Construction and Frost Effects Laboratory (ACFEL)* of the U.S. Army Engineer Division, New England, for the U.S. Army Snow, Ice and Permafrost Research Establishment (USA SIPRE)*. The data collected in each of the three phases of the comprehensive study have been summarized in ACFEL Technical Reports 40 (SIPRE Report 8), 44 (unpublished), and 48 (unpublished). The complete investigation involved the following major topic areas, of which the present summary report covers one: temporary compressive strength, temporary tensile strength, temporary shear strength, ice crystal structure, plastic deformation, dynamic moduli, overall evaluation of physical properties, and, a system for description and classification of frozen soils.

Investigations were in part funded under the continuing Military Construction Investigations (MCI) program conducted for the Engineering Division, Directorate of Military Construction, Office, Chief of Engineers and administered by the Civil Engineering Branch (Mr. T.B. Pringle, Chief). This report was published under DA Task 1T062112 A13001, *Cold Regions Research – Applied Research and Engineering.*

The study was performed under the general direction of Mr. K.A. Linell, Chief, ACFEL (presently Chief, Experimental Engineering Division, CRREL) and Mr. J.F. Haley, Assistant Chief, ACFEL, and the direct supervision of Mr. C.W. Kaplar, Project Engineer (presently Research Civil Engineer, CRREL).

The author wishes to acknowledge the contribution of Dr. Francis Birch, Department of Geology, Harvard University, who designed and constructed the magnetic vibrator used in this study. Grateful acknowledgement is also extended to Mr. O.W. Simoni, Soils Engineer (presently Assistant Chief, Alaska Field Station, CRREL) for the preparation and freezing of the test specimens, and to Mr. M. Levey, Geologist, who performed most of the tests.

Lieutenant Colonel John E. Wagner was the Commanding Officer/Director of the U.S. Army Terrestrial Sciences Center* during the publication of this report, and Mr. W.K. Boyd was Chief Engineer.

USA TSC is a research activity of the Army Materiel Command.

* ACFEL was merged with SIPRE in 1961 to form the U.S. Army Cold Regions Research and Engineering Laboratory (USA CRREL), now an element of the U.S. Army Terrestrial Sciences Center (USA TSC), Hanover, New Hampshire.

CONTENTS

	Page
Preface	ii
Abstract	iv
Introduction	1
Background	1
Definitions	1
Notation	2
Investigations performed	3
Materials	3
Test equipment	3
Preparation and freezing of specimens	9
Molding of specimens	9
Thermocouples	9
Saturation of specimens	9
Placing trays in freezing cabinet	10
Specimen freezing procedure	10
Preparation of frozen specimens for testing	10
Test procedures	13
Test results and discussion	15
Conclusions	23
Selected bibliography	24
Appendix A: Test results	

ILLUSTRATIONS

Figure		
1.	Grain size distribution	5
2.	Electromagnetic three-mode beam vibrator	6
3.	Apparatus used in tests for dynamic modulus	7
4.	Specimen of McNamara concrete sand showing permanent bar magnets frozen flush with end of beam	7
5.	Horizontal beam tray	8
6.	Vertical beam tray	8
7.	Typical beam of undisturbed Boston blue clay frozen in horizontal position	8
8.	Typical beam of undisturbed Boston blue clay frozen in vertical position	8
9.	Typical temperature and heave data for each tray of specimens	11
10.	Summary of data presented on Figures A1-A14	16
11.	Comparison of dynamic modulus E of ice obtained by various investigators	18
12.	Summary of longitudinal or P-wave velocities in ice measured by various investigators	18
13.	Relationship of soil type and dynamic modulus, E_L, at 20F	22

TABLES

I.	Materials tested	3
II.	Summary of soil characteristics	4
III.	Tabulation of specimen data for dynamic modulus tests	12
IV.	Summary of dynamic modulus tests	17
V.	Comparison of propagation velocities of dilatational sonic waves in frozen ground	19

ABSTRACT

This report presents a summary of results of laboratory investigations of frozen soils and ice to determine the elastic moduli by the dynamic (sonic) method. The elastic moduli were indirectly obtained by measuring the fundamental resonant frequencies of flexural, longitudinal, and torsional vibrations induced in prismatic beams by electromagnetic means. Vibration tests were performed on a total of 56 specimens representing 12 different materials (8 natural soil types, ranging from coarse-grained to fine-grained; 2 blended soils; a natural peat; laboratory-frozen ice and natural lake ice, at temperatures ranging from approximately +32F to −10F). Elastic wave velocities (longitudinal and torsional) were computed for each material in the range of test temperatures studied. All soils were saturated or were close to saturation.

The dynamic moduli of elasticity of the frozen soils were found to increase with a decrease in temperature, the greatest rate of increase occurring between +32F and +20F. Coarse granular soils gave the highest values and clays the lowest in the ratio of more than 4 to 1. Dynamic Young's modulus, E, computed from flexural vibrations was usually lower than dynamic E computed from longitudinal vibrations. Average values of dynamic Poisson's ratio for all soil types computed from average values of E and G (longitudinal vibrations) ranged from 0.26 to 0.38. Values of Poisson's ratio for the various soil types did not conform to any logical pattern related to temperature or soil type.

The dynamic moduli of elasticity of ice showed only slight dependence on temperature, and test values were more consistent than those of the soils. Natural lake ice was least temperature dependent and gave the most consistent results. Dynamic moduli of ice E (longitudinal vibration) and G compared closely with values reported by other investigators. Average values of Poisson's ratio for ice were reasonable but less consistent, ranging from 0.30 to 0.41.

LABORATORY DETERMINATION OF THE DYNAMIC MODULI OF FROZEN SOILS AND OF ICE

by

Chester W. Kaplar

I. INTRODUCTION

Background

The determinations of the elastic properties of frozen soils and of ice were made as part of studies of strength properties of frozen soils (ACFEL, 1954; ACFEL, 1952). The elastic properties of frozen soils have not been extensively studied, but several investigators (Boyle *et al.*, 1931; Ewing *et al.*, 1934b; Kornfeld *et al.*, 1942; Lagutin *et al.*, 1946; Nakaya, 1959; Northwood, 1947; Tsytovich *et al.*, 1936, 1937) have measured the elastic properties of ice. In this study tests were conducted on both media, to obtain needed data and facilitate comparison between the two. In these laboratory investigations, dynamic methods were used in non-destructive tests. Vibrations were induced in beams of frozen soil and ice by electromagnetic means. That such dynamic methods are more suitable than static methods for determining elastic properties is supported by many investigators (Wilson *et al.*, 1948; Boyle *et al.*, 1931; Dorsey, 1940; Ewing *et al.*, 1934a). The *static method* usually involves measurements in the plastic rather than the elastic range of deformation. Elastic deformation takes place over such a small range of load and deformations that extremely small stresses must be used, and the deformations within the elastic range are so small that their measurement is difficult and subject to considerable error (Butkovich and Landauer, 1960).

The *dynamic method* is an indirect procedure relating sonic resonant frequencies to the elastic properties of the material. By its use, the large aberrations caused by plastic deformation can be avoided. In the field, velocities of elastic waves produced by buried explosive charges may be measured directly. In the laboratory, longitudinal and transverse wave velocities may be computed from the resonant frequencies induced in small beams of frozen soil and of ice.

It is hoped that the results of these studies will be useful in seismic applications in permafrost regions for possible identification of frozen subsurface strata and in the design of foundations of critical structures subjected to vibrating or oscillating loads. Data from these tests have been useful in the design of radar foundations in permafrost.

Definitions

Elasticity. Elasticity is the property of a strained body by which it returns to its initial size and shape after release of load causing the strain. The body is considered to be *perfectly elastic* if it recovers its original size and shape completely after unloading; it is *partially elastic* if the deformation produced by external forces does not disappear completely after unloading.

Modulus of elasticity (Young's modulus). Young's modulus of elasticity is the rate of change of unit direct stress with respect to unit direct strain (based on original length) for the condition of uniaxial stress within the proportional limit.

Modulus of rigidity (modulus of elasticity in shear or in torsion). Modulus of rigidity is the rate of change of unit stress with respect to unit shear strain, for the condition of pure shear within the proportional limit.

Plastic deformation. Plastic deformation is non-elastic deformation of the material under load; i.e., it is non-recoverable when the load is removed.

Poisson's ratio. Poisson's ratio is the ratio of lateral unit strain to longitudinal unit strain, under the condition of uniform and uniaxial longitudinal stress within the proportional limit.

Degree of saturation. The ratio, expressed as a percentage, of the volume of water (or of ice) in a given soil mass to the total volume of voids.

Frost heave. The raising of a surface due to the formation of ice in the underlying soil (see *Percent heave,* below).

Frost-susceptible soil. A soil in which significant ice segregation will occur (usually in the form of lenses) when certain moisture and freezing temperatures are present.

Percent heave. The ratio, expressed as a percentage, of the amount of heave to the depth of frozen soil before freezing.

Ice content. The ratio, expressed by weight or volume, of the amount of ice in a frozen soil to the amount of dry soil. If by weight, the weight of the ice phase compared to the weight of dry soil, preferably expressed as a percentage; thus, if all moisture is frozen, ice content *by weight* is exactly equal to water content. If by volume, the volume of the ice compared to the volume of soil solids, expressed as a decimal.

Ice segregation. The growth of ice as distinct lenses, layers, veins, or masses in soils – commonly, but not always, oriented normal to the direction of heat loss.

Void ratio. The ratio of the volume of voids to the volume of soil solids in a given soil mass.

Water content. The ratio, expressed as a percentage, of the weight of water in a specimen to the weight of dry soil. In this report, the water content of a frozen soil includes water in the form of ice and any non-frozen water present.

Notation

C	A factor depending upon the shape and size of the specimen, mode of vibration and Poisson's ratio (Pickett, 1945)
E_f	Young's modulus of elasticity derived from flexural vibrations
E_L	Young's modulus derived from longitudinal vibrations
G	Modulus of rigidity (elastic modulus in torsional vibrations)
f_f, f_L, f_t	Fundamental resonant frequency corrected for mass of magnets
f'_f, f'_L, f'_t	Observed fundamental resonant frequency
g	Gravitational acceleration (386 in./sec^2)
i	Number of nodes
k	Ratio of radius of gyration of magnet to that of specimen (used in frequency correction formula for torsional vibrations)
L	Length of specimen
M	Weight of magnets
R	A geometrical factor used in torsion theory (Pickett, 1945)
V	Velocity of wave propagation
w	Unit weight of specimen
W	Total weight of specimen
μ	Poisson's ratio

Subscripts f, L, and t refer to flexural, longitudinal and torsional vibrations, respectively.

II. INVESTIGATIONS PERFORMED

Materials

Table I lists the materials investigated, the number of specimens of each material tested, and the orientation of the beams during unidirectional freezing.

Table I. Materials tested.

Material	*Symbol*	*Number of specimens tested*	
		Frozen horizontally	*Frozen vertically*
Peabody gravelly sand (minus 3/4-in. mesh)	SP	2	0
McNamara concrete sand	SM	1	1
Blend, McNamara concrete sand and East Boston till	SMT	0	5
Blend, Manchester fine sand and East Boston till	SNHT	0	5
East Boston till*	SEBT	0	5
New Hampshire silt	SNHS	2	1
Fairbanks silt	SFS	0	5
Yukon silt	SYS	0	5
Boston blue clay (undisturbed)	SBC	6	0
Fargo clay (undisturbed)	SFFC	5	0
Alaskan peat (undisturbed)	SAP	1	1
Ice, laboratory-frozen	SI	6	4
Ice, natural†	SI-(P)	1	0

* Four specimens consisted of materials passing the No. 4 mesh sieve and one specimen of material passing the 3/4-in. sieve.

† Specimen obtained from large beam cut from natural lake ice at Portage Lake, Maine, in March 1953.

Specimens of Fargo (North Dakota) clay, Boston (Massachusetts) blue clay, and Alaskan (Fairbanks) peat were cut from undisturbed chunks; all specimens of other soils were remolded in the laboratory. From two to ten specimens of each material were tested at various temperatures ranging from approximately +32F to -10F. The grain size distributions of the soils used are shown in Figure 1. A complete summary of soil characteristics and sources will be found in Table II.

Test equipment

Dynamic modulus test apparatus. The principal items of equipment used in this investigation are shown in Figures 2 and 3. The complete apparatus consisted of a variable frequency oscillator capable of producing frequencies from 18 to 220,000 cycles per second, an amplifier, a cathode-ray oscilloscope, a vacuum tube voltmeter, and a magnetically coupled specimen vibrating apparatus and detector. The magnetically coupled vibrator was designed and constructed for this study by Dr. Francis Birch of Harvard University. Beams having dimensions of approximately 1½ x 1½ x 11 in. were used in the investigation. The vibrator, however, can accomodate beams up to 2¼ in. square in cross section.

Permanent bar magnets, $^3/_{16}$ x $^3/_{16}$ x 2 in., were frozen flush into horizontal grooves prepared in each end of the frozen specimen beams with the ends of the magnets protruding ¼ in. on each side (Fig. 4). Vibration of the specimens was actuated by two oscillating magnetic fields from a pair of electromagnets mounted in series at one end of the apparatus. Each electromagnet consisted of very fine wire wound around a C-shaped laminated core. The air gaps between the poles of the magnets were ¼ in., sufficient to accommodate the $^3/_{16}$ in. thick bar magnets without touching.

TABLE II

SUMMARY OF SOIL CHARACTERISTICS

SOIL LEGEND	NAME	SOURCE	DEPARTMENT OF THE ARMY UNIFIED SOIL CLASSIFICATION *		ATTERBERG LIMITS			SPECIFIC GRAVITY	COMPACTION CHARACTERISTICS		TYPICAL PROPERTIES OF SPECIMENS (before freezing)	
			DESCRIPTION	GROUP SYMBOL	LIQUID LIMIT	PLASTICITY INDEX	SHRINKAGE LIMIT		MAX. DRY UNIT WT. (pcf)	OPTIMUM WATER CONTENT (percent)	DRY UNIT WT. (pcf)	VOID RATIO
SP	Peabody Gravelly Sand	Peabody, Mass.	Bank run gravelly SAND	SP	non-plastic		-	2.72	134 (1)	-	125	0.356
SM	McNamara Concrete Sand	Needham, Mass.	SAND, brown, angular, processed for concrete	SP	non-plastic		-	2.72	123 (1)	-	117	0.456
SMT	Blend, McNamara Concrete Sand and East Boston Till	SM Blended with 35% minus 40 mesh SEBT	Silty SAND	SM	non-plastic		-	2.72	142 (2)	6.8	135	0.262
SNHT	Blend, Manchester Fine Sand and East Boston Till	SNH Blended with 35% minus 40 mesh SEBT	Silty SAND	SM	non-plastic		-	2.72	128 (2)	9.2	121	0.398
SEBT	East Boston Till (-3/4")	East Boston, Mass.	Clayey, gravelly SAND (Glacial Till)	SC	21	7	-	2.76	137 (2)	8.1	130	0.327
SNHS	New Hampshire Silt	Manchester, N. H.	Light gray brown, inorganic clayey SILT	CL-ML	26	5	-	2.70	107 (2)	15.6	102	0.653
SFS	Fairbanks Silt	Fairbanks, Alaska	Brown and gray SILT, containing traces of mica and some organic matter	ML-OL	28	4	-	2.68	112 (2)	15.7	105	0.590
SYS	Yukon Silt	Whitehorse, Yukon Territory, Canada	Gray, well graded, inorganic clayey SILT	CL-ML	28	9	-	2.73	121 (3)	12.8	115	0.479
SBC	Boston Blue Clay	No. Cambridge, Mass.	Stiff lean CLAY, relatively homogeneous and free of fractures and varves	CL	47	27	22	2.81	-	-	85	1.057
SFFC	Fargo Clay	Fargo, North Dakota	Dark gray, friable, highly plastic homogeneous fat CLAY, with honeycomb structure (organic content 8%)	CH-OH	68	46	15	2.76	-	-	87	0.980
SAP	Alaskan Peat	Fairbanks, Alaska	Dark brown to black PEAT; fibrous, partially decomposed (organic content 82 percent)	Pt	Tests inapplicable			1.52	-	-	-	-

NOTES: (1) Providence Vibrated Density (Proc. 2nd Int. Conf. on Soil Mech. and Fdn. Engineering, v. 4, p. 243)
(2) Modified AASHO Density (ASTM T180-57D)
(3) Standard Proctor Density (ASTM T99-57A)

* Technical Memorandum No. 3-357, Waterways Experiment Station, Vicksburg, Mississippi, vol. 1, Mar. 1953.

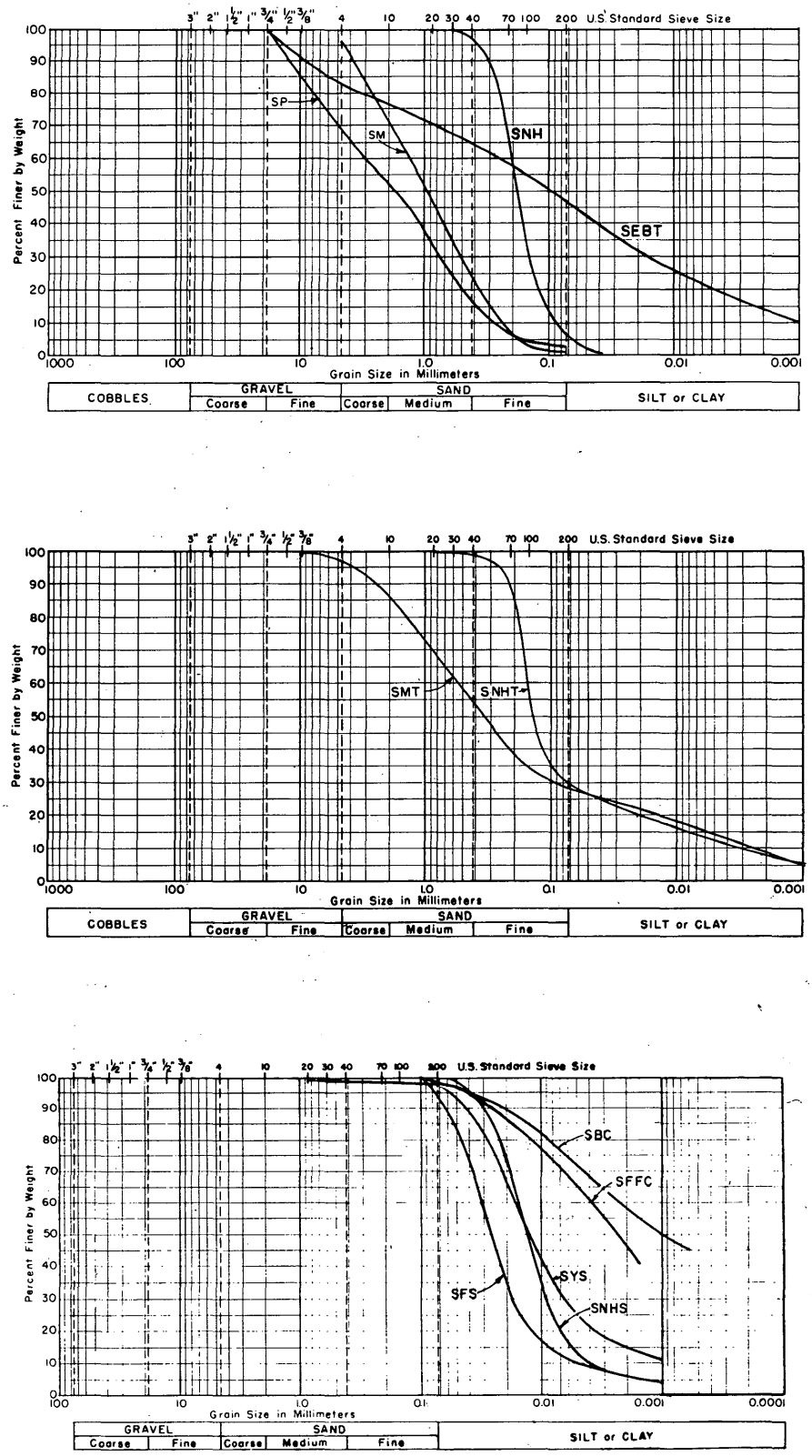

Figure 1. Grain size distribution. See Table I for soil names.

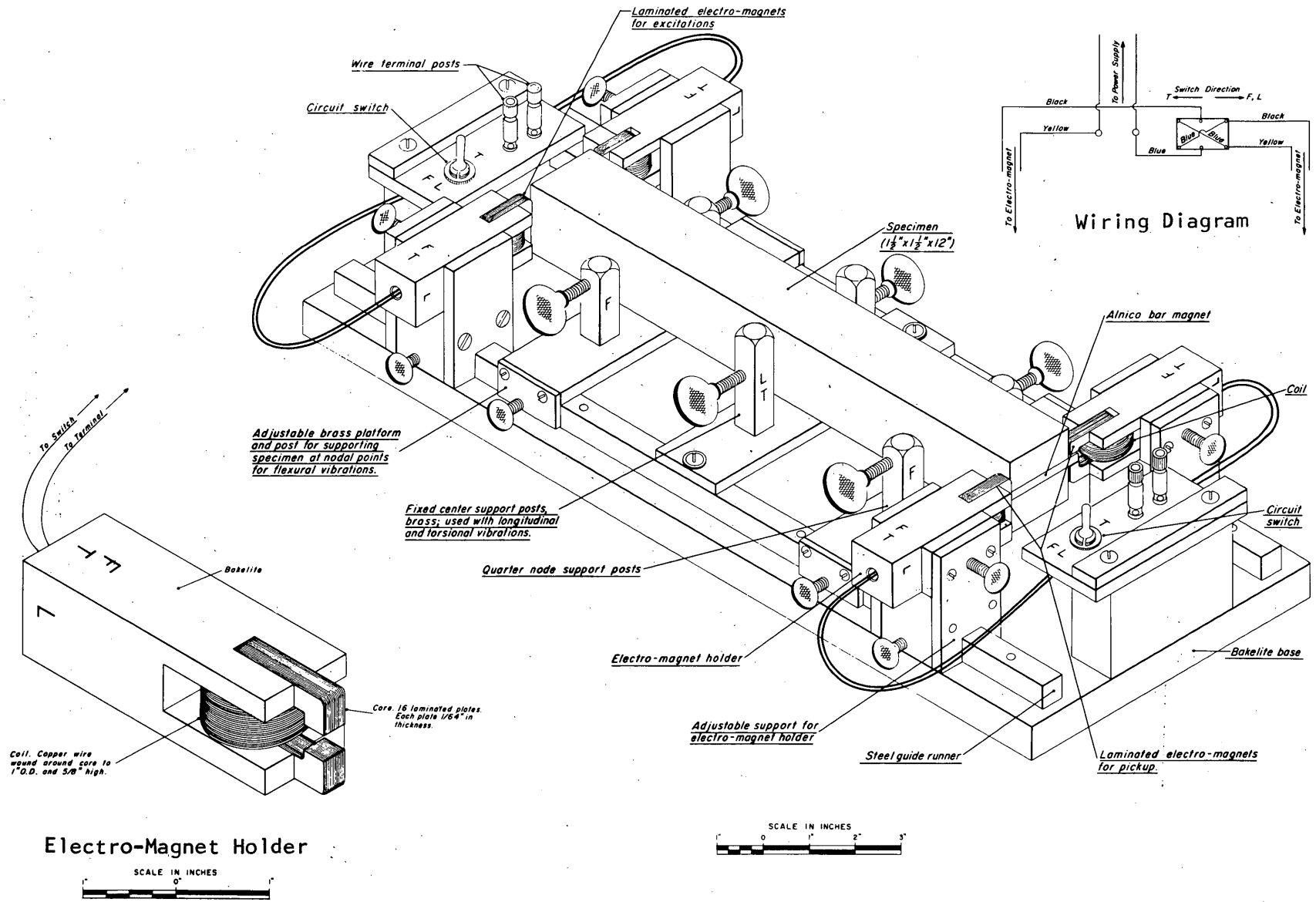

Figure 2. Electromagnetic three-mode beam vibrator (for flexural, longitudinal and torsional vibrations).

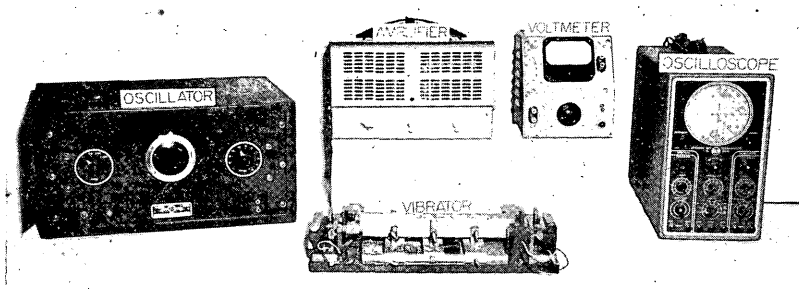

Figure 3. Apparatus used in tests for dynamic modulus.

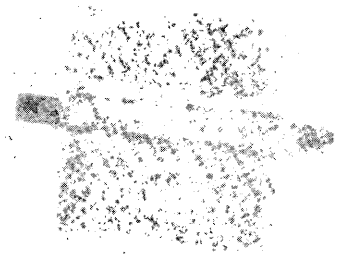

Figure 4. Specimen of McNamara concrete sand showing permanent bar magnets frozen flush with end of beam.

The electromagnets were held in horizontally and vertically adjustable supports and could lie in either a horizontal or a vertical plane. A switching arrangement was provided to enable corresponding poles of each electromagnet to be of the same or of opposite polarity. The arrangement of the two detector magnets on the other end of the apparatus was the same as on the driving end.

Freezing trays. Two wooden molding trays were used in the preparation and freezing of the soil beams used in the investigation. Each was constructed of white oak and treated to resist moisture absorption. One of the trays contained six horizontal compartments, 1½ x 4½ x 12 in., for horizontally positioned soil beams (Fig. 5). Since freezing was from top to bottom the ice lenses* in these specimens formed in a direction parallel to the longitudinal axis of the beam (Fig. 7). The specimens molded in this tray are identified by the prefix HB (Horizontal Beam). The other tray (Fig. 6) contained 25 vertical compartments, 1½ x 1½ x 12 in., for the preparation of beams to be frozen in a vertical position, i.e., beams in which ice lenses formed in planes normal to the longitudinal axis of the beam (Fig. 8). The samples molded in this tray are identified by the prefix VB (Vertical Beam).

Both types of trays were constructed of removable sections to facilitate dismantling and removal of frozen specimens. Along the top and bottom edges of each tray there was provided a continuous rubber gasket, ¼ in. thick and 1½ in. wide, and a series of ¼-in. stud bolts for attaching watertight covers made of 11-gage galvanized sheet steel. Top and bottom covers each contained a ¼-in. brass nipple 3 in. long in the center, for attaching de-airing and saturating apparatus. When the trays were assembled and filled with test beams, a ¼ in. thick filter mat was placed on both top and bottom within the space provided by the thick rubber gasket. These mats were built up from 64 x 64 weave muslin (next to specimens), 18 x 14 mesh bronze screen cloth and ½-in. 18-gage galvanized expanded metal. The filter mats and covers were used during the simultaneous evacuation and saturation of all the specimens in the tray prior to freezing. The top cover and mat were removed during the freezing of the specimens. Sample preparation and freezing procedures are described below.

* Note that the reference here is to ice lenses, not crystal optic axes.

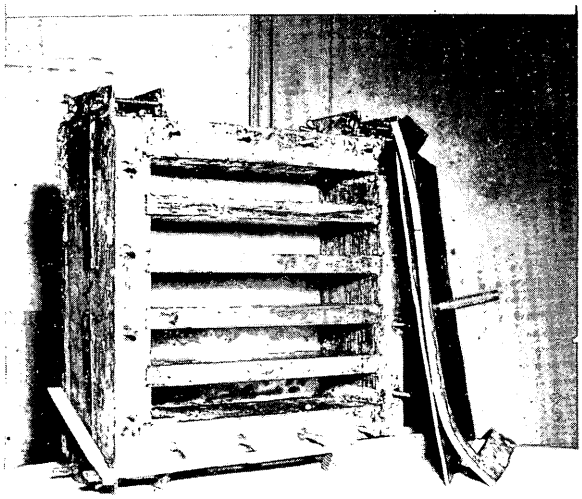

Figure 5. Horizontal beam tray.

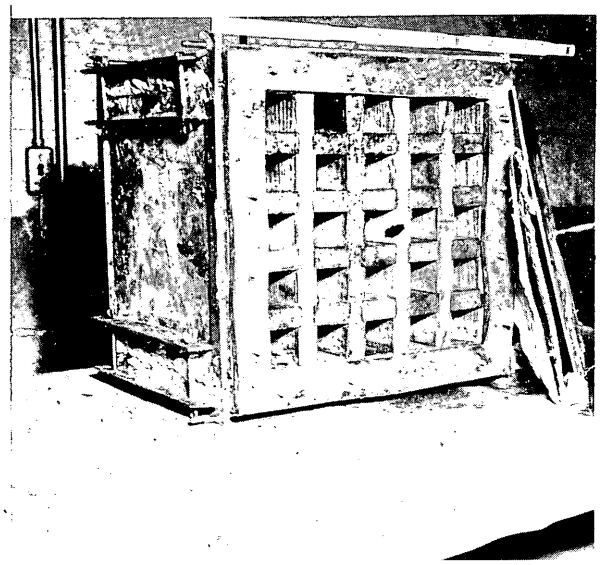

Figure 6. Vertical beam tray.

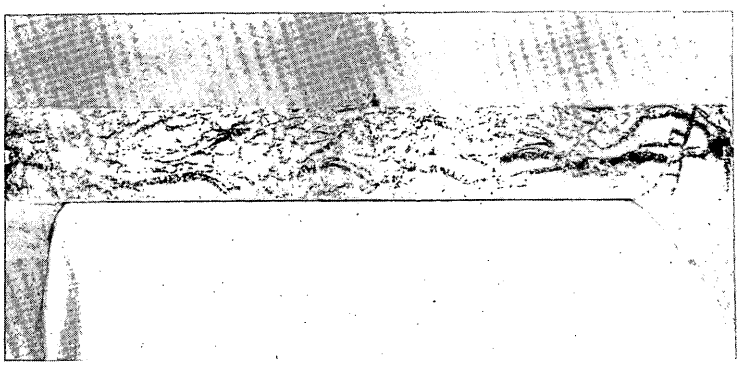

Figure 7. Typical beam of undisturbed Boston blue clay frozen in horizontal position. Ice lenses oriented horizontally, parallel to longitudinal axis of beam. Note magnets in ends of sample.

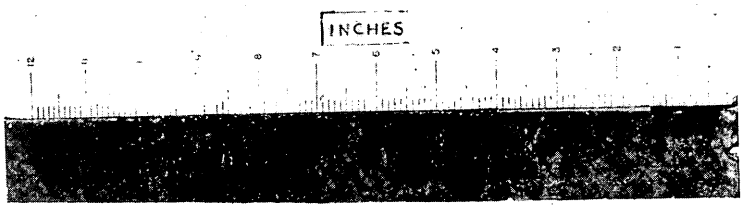

Figure 8. Typical beam of undisturbed Boston blue clay frozen in vertical position. Ice lenses oriented perpendicular to longitudinal axis.

III. PREPARATION AND FREEZING OF SPECIMENS

Molding of specimens

With the exception of the undisturbed materials, i.e., Boston blue clay, Fargo clay, and Alaskan peat, the test soils were molded at optimum water content* to densities approximately 95% of the maximum determined by the Providence Vibrated Density Test (Lane, 1948) for the cohesionless soils, i.e., Peabody gravelly sand and McNamara concrete sand, and the Modified AASHO Tests, ASTM T180-57D or ASTM T99-57A for the other soils.

Before the soil was placed in the freezing trays, the inside walls of the wooden molds were lubricated with a thin coating of petrolatum and lined with transparent cellulose acetate, 0.007 in. thick. The petrolatum and acetate served to minimize the side friction of frost-susceptible specimens during the period of heave and facilitated the removal of frozen specimens from the molds. With the bottom filter mat in place between the bottom cover and the mold, the bottom cover was secured tightly against the rubber gasket by means of the studs, nuts and washers. The specimens were then either compacted or inserted into the molds.

Generally, two individual soil beams were obtained from each 4½ in. deep compartment of the horizontal beam tray. With the filter mat and the bottom cover plate in place, a known quantity of soil was uniformly placed and compacted to a depth slightly over 1½ in. Next a ¾-in. layer of Ottawa sand was deposited, and over this material another beam of soil was compacted in place. The ¾-in. space remaining between the top layer of soil and the top of the mold was filled with Ottawa sand. The top filter mat and cover were then put in place and fastened.

For the undisturbed clays and peat, horizontal beams or segments 1½ in. wide and 4½ in. deep were cut to size from a large undisturbed chunk sample from a horizontal section, oriented in the same position as in the field.

The preparation of remolded specimens in the vertical beam tray consisted of placing the soil in the vertical compartment in thin layers and compacting with a 1¼ in. square wood block. Except for only one specimen of Alaskan peat, no vertical beams were cut from undisturbed field chunks because of difficulties in manipulating such slender specimens (1½ x 1½ x 12 in.).

Thermocouples

In at least one specimen in each tray, copper-constantan thermocouples were placed at approximately 2-in. vertical intervals or closer, as an aid in the regulation of the rate of freezing. Other thermocouples were placed at the top and bottom of some specimens for assurance that freezing had taken place in all parts of the tray.

Saturation of specimens

Before freezing, the specimens in the tray were de-aired and then saturated in a +40F cold room. After de-airing by use of a vacuum at top and bottom via the nipples on the cover plates, water was admitted at the bottom while the de-airing process was continued at the top. The procedure was continued for a minimum of 12 hours for the non-frost-susceptible soils (cohesionless sands and gravels) and 24 hours or longer for all the other soils, until the discharge of water at the top of the tray was virtually free from air. During the saturation process, the specimens had cooled to approximately 40F prior to being placed in the freezing cabinets.

---

* The water content for which maximum density is obtained for a given compactive effort.

Placing trays in freezing cabinet

After saturation was completed the specimen trays were placed in the freezing cabinets within the +40F cold room. The top metal cover and mat were then removed and thin aluminum plates were placed over each specimen to prevent sublimation. A source of de-aired water was connected through a constant-feed water level device to the brass nipple on the bottom cover plate and the water-control device was adjusted to maintain the elevation head at the level of the tops of the specimens during freezing. The space between the tray and the walls of the cabinet was insulated with granulated cork to confine heat flow to the vertical direction.

Specimen freezing procedure

Specimens were frozen unidirectionally from top to bottom, with the bottom of the trays exposed to a temperature of approximately +38 to 40F. Freezing was initiated by lowering the air temperature in the freezing cabinet to approximately +15F, until crystallization was observed in the uppermost part of the specimen. The cabinet temperature was then raised to +29F by resetting the thermoregulator and leaving the cover of the cabinet open for a short period of time, usually 20-30 minutes, to warm up the chamber. Thereafter, the cabinet air temperature was reduced daily by successively larger decrements as necessary to freeze the specimens uniformly in the time required – at a rate ranging from approximately ½ to ¾ in. per day. Trays containing ice specimens were given one extra day of freezing at the end to ensure that the specimens were completely frozen. Temperatures within the specimens were read daily and temperatures in the cabinets were adjusted accordingly, depending upon the progress of the 32F isotherm within the specimens. The heave of each specimen was measured daily to the nearest half-millimeter. Measurements were obtained by scale readings at the intersection of a meter stick placed vertically on the metal plates on the top of the specimens and a metal bar placed across the cabinet opening. Figure 9 illustrates typical temperature and heave data obtained during freezing.

Preparation of frozen specimens for testing

After freezing, the specimens were removed by carefully dismantling the tray. The appearance and a brief description, including size and frequency of ice lenses, were recorded. Each specimen was trimmed to uniform dimensions, measured, weighed, and tempered for a period of at least 16 hours at each test temperature before sonic testing. A tabulation of the pertinent data obtained for each specimen is presented in Table III.

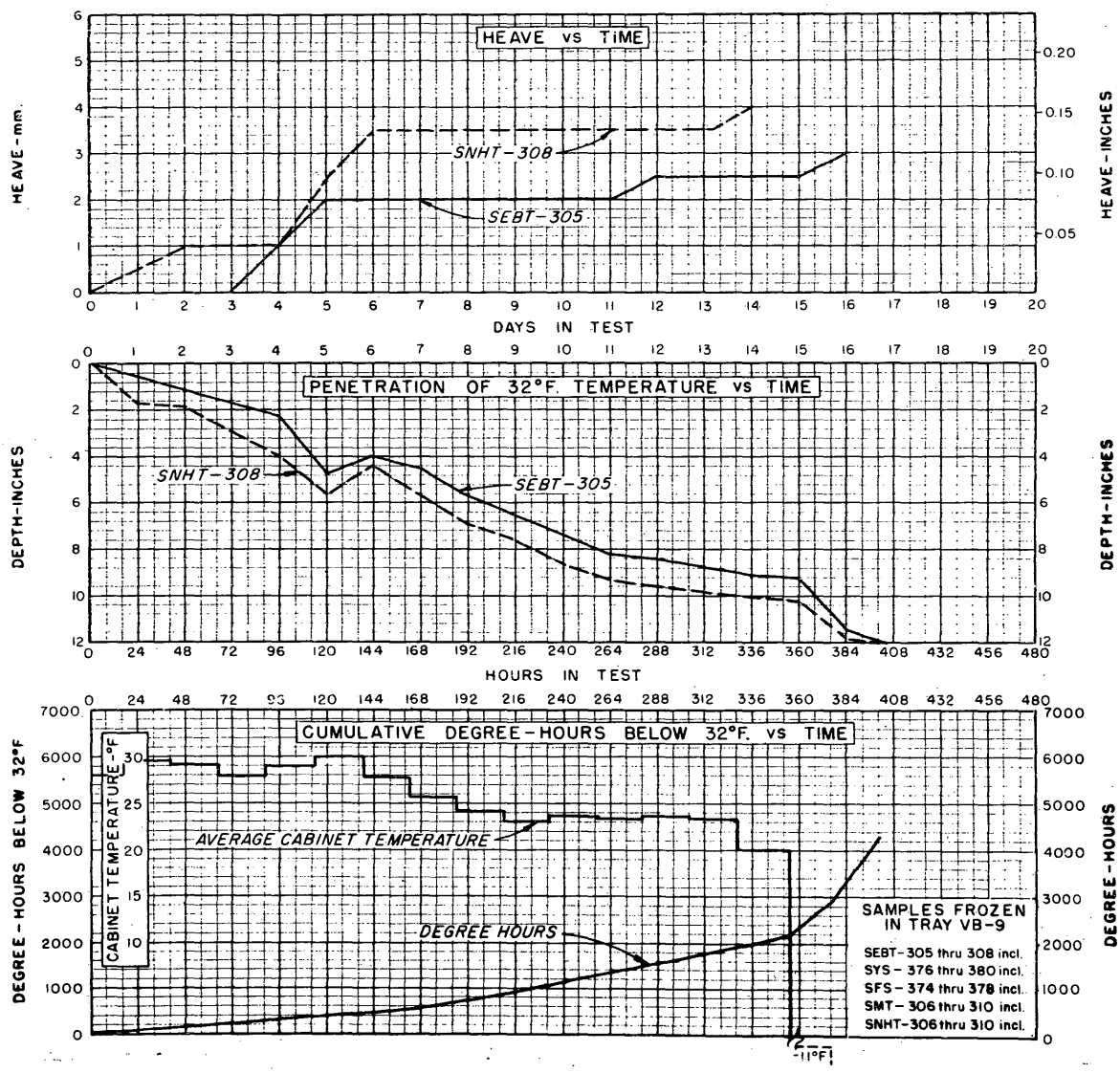

Figure 9. Typical temperature and heave data for each tray of specimens.

TABLE III

TABULATION OF SPECIMEN DATA FOR DYNAMIC MODULUS TESTS

MATERIAL	SPECIMEN NUMBER	TRAY NUMBER	APPROX. RATE OF FREEZING inch/day	POSITION IN TRAY DURING FREEZING (1)	LENGTH OF SPECIMEN in. (2)	AVERAGE SPECIMEN AREA sq. in. (2)	TOTAL WET WEIGHT lb. (2)	WET UNIT WEIGHT AFTER FREEZING pcf (2)	DRY UNIT WEIGHT AFTER FREEZING pcf (3)	WATER CONTENT AFTER FREEZING %	DEGREE OF ICE SATURATION % (4)	VOID RATIO e	RATIO: VOL. ICE / VOL. SOIL (5)
Peabody Gravelly Sand (-3/4 inch size only)	SP-300	HB-11	0.50	U	12.03	2.52	2.267	129	113	14.5	85	0.503	0.430
	SP-301	HB-11	0.50	L	11.86	2.43	2.188	131	116	12.7	81	0.464	0.377
McNamara Concrete Sand	SM-154	HB-3	0.50	U	12.00	2.22	1.978	128	113	13.6	80	0.503	0.403
	SM-200	VB-2	0.50	-	11.84	2.26	2.067	133	117	13.9	91	0.452	0.412
Blend, McNamara Concrete Sand and East Boston Till	SMT-306	VB-9	0.75	-	11.00	2.46	2.130	136	118	15.1	100	0.439	0.448
	SMT-307	VB-9	0.75	-	11.00	2.23	2.008	141	124	14.2	100	0.369	0.421
	SMT-308	VB-9	0.75	-	11.00	2.28	2.077	143	127	12.5	100	0.337	0.371
	SMT-309	VB-9	0.75	-	11.00	2.28	2.068	142	127	12.2	100	0.337	0.362
	SMT-310	VB-9	0.75	-	10.95	2.58	2.284	140	125	12.1	97	0.369	0.359
Blend, Manchester Fine Sand and East Boston Till	SNHT-306	VB-9	0.75	-	10.93	2.66	2.227	133	119	12.3	85	0.427	0.365
	SNHT-307	VB-9	0.75	-	11.03	2.45	2.004	128	115	13.1	81	0.477	0.389
	SNHT-308	VB-9	0.75	-	10.95	2.29	1.962	135	118	13.9	94	0.439	0.412
	SNHT-309	VB-9	0.75	-	10.93	2.34	1.973	133	116	13.2	84	0.464	0.392
	SNHT-310	VB-9	0.75	-	11.05	2.71	2.273	131	117	14.1	93	0.451	0.418
East Boston Till	SEBT-304 *	VB-9	0.75	-	11.06	2.67	2.337	137	125 †	11.2 ††	89	0.378	0.337
	SEBT-305 *	VB-9	0.75	-	11.05	2.31	2.145	145	133	7.0	71	0.295	0.211
	SEBT-306 *	VB-9	0.75	-	10.99	2.32	2.123	144	131	9.4	90	0.315	0.283
	SEBT-307 *	VB-9	0.75	-	10.99	2.31	1.936	132	127	5.7	48	0.357	0.172
	SEBT-308 **	VB-9	0.75	-	11.08	2.59	2.388	144	129	12.2	100	0.336	0.367
New Hampshire Silt	SNHS-150	VB-2	0.50	-	11.52	2.21	1.610	109	77	41.5	100	1.190	1.222
	SNHS-152	HB-3	0.50	U	12.00	2.24	1.700	109	85	28.1	84	0.984	0.827
	SNHS-153	HB-3	0.50	L	12.00	2.27	1.760	112	85	31.4	94	0.984	0.925
Fairbanks Silt	SFS-374	VB-9	0.75	-	11.00	2.44	1.850	119	94	26.5	99	0.780	0.775
	SFS-375	VB-9	0.75	-	11.00	2.29	1.800	123	100	23.0	100	0.673	0.672
	SFS-376	VB-9	0.75	-	11.00	2.32	1.852	125	104	20.5	98	0.609	0.599
	SFS-377	VB-9	0.75	-	11.00	2.36	1.856	124	102	21.5	98	0.640	0.628
	SFS-378	VB-9	0.75	-	11.00	2.58	2.017	123	99	23.7	100	0.690	0.693
Yukon Silt	SYS-376	VB-9	0.75	-	11.01	2.44	1.962	126	102	22.9	100	0.671	0.682
	SYS-377	VB-9	0.75	-	11.03	2.23	1.847	130	106	22.3	100	0.608	0.664
	SYS-378	VB-9	0.75	-	11.01	2.25	1.869	130	109	20.1	100	0.563	0.598
	SYS-379	VB-9	0.75	-	11.09	2.28	1.925	132	110	19.8	100	0.549	0.589
	SYS-380	VB-9	0.75	-	10.93	2.62	2.081	126	105	20.2	96	0.623	0.601
Boston Blue Clay (Undisturbed)	SBC-307	HB-11	0.50	M	10.77	2.28	1.416	100	65	54.1	98	1.698	1.658
	SBC-307A	HB-11	0.50	U	10.70	2.28	1.546	110	80	37.2	95	1.193	1.140
	SBC-308	HB-11	0.50	L	10.73	2.26	1.243	88	48	85.0	98	2.654	2.604
	SBC-309	HB-11	0.50	M	10.63	2.28	1.336	95	59	60.8	94	1.973	1.863
	SBC-309A	HB-11	0.50	U	10.61	2.28	1.265	90	52	73.8	95	2.373	2.261
	SBC-310	HB-11	0.50	L	10.63	2.26	1.492	107	76	41.6	97	1.308	1.275
Fargo Clay (Undisturbed)	SFFC-366	HB-11	0.50	M	10.95	2.26	1.589	111	83	33.5	94	1.076	1.008
	SFFC-366A	HB-11	0.50	U	11.08	2.15	1.494	108	81	33.4	89	1.127	1.005
	SFFC-367	HB-11	0.50	L	11.03	2.01	1.402	109	81	35.6	95	1.127	1.072
	SFFC-368	HB-11	0.50	U	10.93	2.19	1.492	108	80	34.5	90	1.154	1.038
	SFFC-369	HB-11	0.50	L	10.99	2.18	1.501	108	80	35.3	92	1.154	1.063
Alaskan Peat (Undisturbed)	SAP-148	VB-2	0.50	-	11.10	2.26	0.904	62	13	371	98	6.302	6.150
	SAP-150	HB-3	0.50	L	11.90	2.12	1.030	71	19	280	100	3.996	4.641
Ice, Artificially Frozen Tap Water	SI-670	HB-10	0.75	U	10.47	2.25	0.761	56	-	-	-	-	-
	SI-671	HB-10	0.75	L	10.45	2.25	0.745	55	-	-	-	-	-
	SI-672	HB-10	0.75	U	10.47	2.22	0.752	56	-	-	-	-	-
	SI-673	HB-10	0.75	L	10.42	2.26	0.750	55	-	-	-	-	-
	SI-674	HB-10	0.75	U	10.51	2.26	0.756	55	-	-	-	-	-
	SI-675	HB-10	0.75	L	10.47	2.31	0.763	55	-	-	-	-	-
	SI-664	VB-4	0.50	-	10.49	2.38	0.783	54	-	-	-	-	-
	SI-665	VB-4	0.50	-	10.51	2.34	0.787	55	-	-	-	-	-
	SI-667	VB-4	0.50	-	10.50	2.28	0.772	56	-	-	-	-	-
	SI-668	VB-4	0.50	-	10.50	2.26	0.765	56	-	-	-	-	-
Ice, Natural - Portage Lake	SI-(P)	-	-	-	9.95	2.24	0.725	56	-	-	-	-	-

Notes: (1) U, M, and L indicate upper, middle, and lower sections, respectively, in freezing tray compartment.
(2) After trimming.
(3) Computed from measured dimensions and dry weight of trimmed specimen.
(4) Ratio of volume of voids filled with ice to total void volume expressed as a percentage. All water assumed frozen.
(5) All water assumed in frozen state.

All specimens supplied with water during freezing.

* Only material passing No. 4 mesh sieve.
** Only material passing 3/4-inch mesh sieve.

† Computed from measured dimensions and dry weight of entire specimen before trimming.

†† Computed from wet weight and dry weight of entire specimen before trimming.

IV. TEST PROCEDURES

The specimens, with bar magnets frozen-in horizontally across each end, were supported by their sides in a horizontal position in the apparatus between pairs of posts with blunt cone-shaped prongs. For longitudinal and torsional vibrations, the beam was supported midway between the ends. For flexural vibrations the beam was supported at the "quarter nodes," a distance from each end equal to 0.224 times the length of the specimen.

The two driving electromagnets were positioned so that each projecting end of the bar magnet embedded in the test beam lay between the poles of an electromagnet.

Since the poles of the electromagnets change polarity with the frequency of the alternating current in the coils, they alternately attract and repel the permanent bar magnet, causing the specimens to vibrate. The position of the two driving electromagnets, the direction of the current in their respective coils, and the position of the specimen support(s) determine the type of vibration that is induced.

For flexural and torsional vibrations, the electromagnets were set so that their poles were in the same vertical plane as the bar magnets on the specimen (Fig. 3). To produce flexural vibrations, the alternating current was made to pass through the coils so as to produce polarities of opposite sign in the corresponding poles of the two driving electromagnets. The resulting simultaneous attraction and repulsion of the bar magnet in an up and down direction caused the beam to vibrate in flexure. To incite torsional vibrations, the beam was supported firmly at its midpoint and current passed through the driving magnets to induce the same polarity simultaneously in corresponding poles of both driving magnets. This caused the specimen to vibrate in torsion about its longitudinal axis. Longitudinal vibrations were produced with the poles of the electromagnets placed in a horizontal plane, with corresponding poles having opposite polarity, the specimen being supported at the midpoint. The effect was alternately to push and pull on the bar magnet in a horizontal plane, parallel to the longitudinal axis of the specimen.

The permanent bar magnet at the opposite end of the beam was caused to vibrate at the same frequency and the fluctuations of the magnetic field induced an electromotive force of varying intensity in the receiving or detecting coils. In theory, the peak voltage is induced when the specimen is vibrating at its natural frequency and the amplitude of the vibrations is then at a maximum. The fundamental resonant frequency was detected with a vacuum tube voltmeter and/or a cathode-ray oscilloscope connected to the detecting coils, and read from the dial markings of the calibrated oscillator. Peak readings on the voltmeter and oscilloscope were also obtained from overtones or harmonics of the fundamental frequency. In the torsional and longitudinal modes, the overtones are nearly integral multiples of the respective fundamental frequencies. In the flexural mode, the frequencies of the first two overtones occur at 2.7 and 5 times the fundamental frequency.

The following equations (Pickett, 1945) were used in the computations:

Flexural vibrations.

$$E_f = CW(f_f)^2 .$$

(A value of $\frac{1}{3}$ was assumed for Poisson's ratio μ to find C from curves given in Pickett, 1945. The value of μ is not critical and the assumption is reasonable.)

Longitudinal vibrations.

$$V_L = 2 f_L L$$

and

$$E_L = \frac{w(V_L)^2}{g} = \frac{4wL^2(f_L)^2}{g}.$$

Torsional vibrations.

$$V_t = 2f_t L$$

and

$$G = \frac{w(V_t)^2 R}{g} = \frac{4\,wL^2R(f_t)^2}{g}$$

[R is 1.183 for a square prism (Pickett, 1945)].

Correction to observed frequencies for mass of magnets (Rayleigh, 1929).

Flexural vibrations: $f_f = f_f'(1 + \frac{2M}{w})$

Longitudinal vibrations: $f_L = f_L'(1 + \frac{M}{w})$

Torsional vibrations: $f_t = f_t'(1 + \frac{K^2M}{w})$

Poisson's ratio. Poisson's ratio is computed from E and G using the relation:

$$\mu = \frac{E}{2G} - 1.$$

It should be remembered that these formulas are strictly applicable only to an isotropic elastic solid complying with Hooke's law.

V. TEST RESULTS AND DISCUSSION

The individual test results for all materials and specimens are presented in Appendix A. Summaries are presented in Table IV and Figure 10. The individual values of moduli of elasticity and rigidity obtained from the measured resonant frequencies are presented in graphs a and c of Figures A1–A14, for each test temperature. The test temperatures ranged from approximately +32F to below -10F. The elastic wave velocities at resonant frequencies for the longitudinal and torsional vibrations are plotted versus temperature in graphs b and d.

Theoretically, for an elastic isotropic homogeneous solid the dynamic modulus of elasticity derived from flexural and longitudinal vibrations should be the same. In most of the present tests the numerical values of E obtained from flexural vibrations were slightly lower than those obtained from longitudinal vibrations. These differences are not surprising since a frozen soil containing irregularly stratified ice lenses cannot truly be considered as isotropic homogeneous material. Only an isotropic material, in which every plane is a plane of symmetry, can be characterized by only two elastic constants such as Young's modulus and Poisson's ratio (Love, 1927).

In graph e of Figures A1–A14 are presented curves of dynamic Poisson's ratio [calculated using the relationship $\mu = (E/2G) - 1$] vs temperature. Average values of dynamic E and G obtained from curves in graphs a and c of Figures A1–A14 were used in the above formula. Of the two sets of data for Poisson's ratio the values computed using longitudinal vibrations are believed more reliable and reference is made to this set when comparing these data.

The plotted data and summary curves in Figure 10 show that dynamic moduli and elastic wave velocities in frozen soils are temperature dependent – more so at temperatures above +20F and less so at colder temperatures. The propagation velocities in the silts and clay appear to be particularly sensitive to temperature changes in the range from +32F to +20F. Below about +20F the velocities increase linearly and are less dependent on temperature. This behavior is due to the varying percentages of non-frozen water believed to be present in the soil at temperatures below freezing (Tsytovich, 1957).

A comparison of laboratory-determined dilatational wave velocities with those obtained in permafrost by seismic refraction methods shows good agreement for comparable soil types as indicated in Table V.

The agreement in Table V varies in some instances, principally because no borings were made in the field work and precise knowledge of the overburden was lacking except from general geologic knowledge of the area.

A comparison of the dynamic moduli of ice obtained during this study with the work of other investigators also reveals very close agreement. The moduli of elasticity computed from results of longitudinal vibrations in these tests are shown plotted on Figure 11 along with other data previously summarized in USA SIPRE Report 8 (ACFEL, 1952).

On Figure 12 are shown plotted the dilatational wave velocities of both laboratory and field seismic data on ice for comparison with the present results. It will be seen here that the laboratory results are compatible with the results of other investigators. The field velocities in ice sheets and ground ice are higher. This is due to the fact that velocities of longitudinal waves in thin bars or rods, in thin plates, and in infinitely extended solids are all different. Available formulas (Ewing, *et al.*, 1934) show that longitudinal velocities in a thin ice plate may be 5 to 10% higher than in thin ice rods, and in extended ice masses the velocities may be 20–25% higher depending upon the value of Poisson's ratio μ used in the formulas. This is borne out by the experimental data presented in Figure 12.

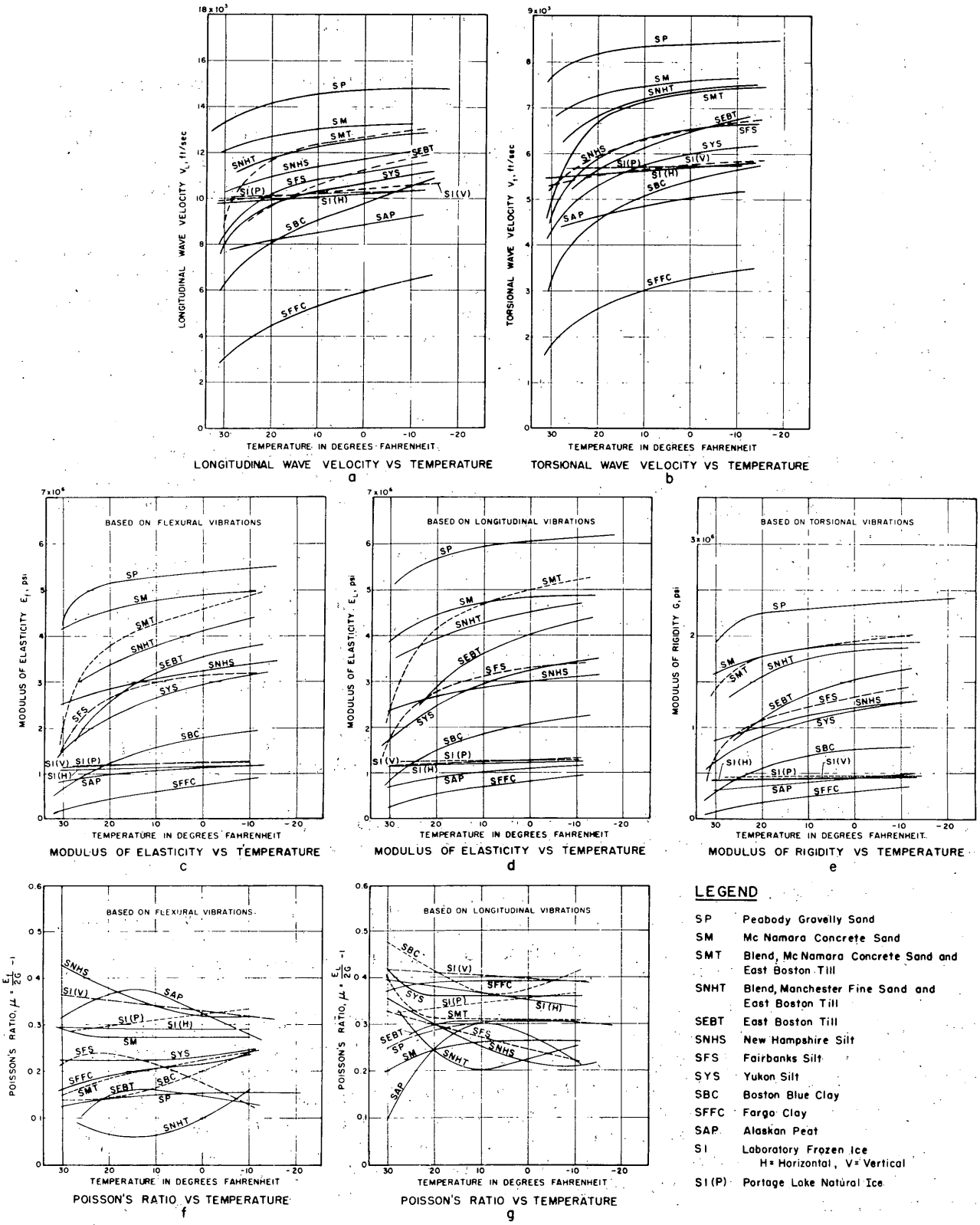

Figure 10. Summary of data presented on Figures A1–A14. Each curve represents test results of two to six specimens. Curves of Poisson's ratio vs temperature are based on values taken from pertinent curves in graphs c, d and e.

TABLE IV

SUMMARY OF DYNAMIC MODULUS TESTS(1)

Material	Symbol	Number of Specimens Tested	Range of Moduli of Elasticity, E, psi x 10^6 (Flexural and Longitudinal)		Range of Moduli of Rigidity, G, psi x 10^6		Range of Velocities, V, ft/sec x 10^3 (Longitudinal)		Range of Velocities, Vt, ft/sec x 10^3 (Torsional)		Poisson's Ratio(2)			
											Flexural		Longitudinal	
			+30°F	-10°F	+30°F	-10°F	+30° F	-10°F	+30° F	-10°F	+30°F	-10°F	+30°F	-10°F
Peabody Gravelly Sand	SP	2	4.2 - 5.2	5.0 - 6.2	1.8 - 2.0	2.3 - 2.4	13.2 - 13.5	14.7 - 14.9	7.4 - 7.8	8.3 - 8.5	0.13	0.16	0.25	0.31
McNamara Concrete Sand	SM	2	3.6 - 4.3	4.8 - 5.1	1.4 - 1.7	1.9 - 2.0	11.4 - 11.9	- - 13.2	6.5 - 7.3	7.5 - 7.7	0.29	0.27	0.20	0.26
Blend, McNamara Concrete Sand and East Boston Till	SMT	5	1.8 - 2.6	4.6 - 5.4	0.8 - 0.9	1.9 - 2.1	8.9 - 9.0	12.6 - 13.1	4.7 - 4.9	7.3 - 7.5	0.15	0.24	0.40	0.31
Blend, Manchester Fine Sand and East Boston Till	SNHT	5	2.7*- 3.5*	4.0 - 4.8	1.4*- 1.6*	1.7 - 1.8	10.8*- 11.0*	12.7 - 12.8	6.0*- 6.3*	7.4 - 7.5	0.10	0.16	0.36*	0.25
East Boston Till	SEBT	5	1.2*- 2.2*	3.2 - 4.4	0.6*- 0.8*	1.4 - 1.8	7.4*- 8.0*	11.5 - 11.9	4.5*- 4.9*	6.4 - 6.9	0.07*	0.13	0.26*	0.30
New Hampshire Silt	SNHS	3	2.4 - 2.8	2.7 - 3.6	0.6 - 1.0	1.2 - 1.3	10.0 - 10.9	10.7 - 11.8	4.8 - 5.8	6.6 - 6.9	0.43	0.32*	0.35	0.21*
Fairbanks Silt	SFS	5	1.3 - 2.0	3.0 - 3.6	0.5 - 0.8	1.3 - 1.5	7.7 - 8.9	11.3 - 11.7	4.5 - 4.7	6.5 - 6.8	0.21	0.14	0.33	0.22
Yukon Silt	SYS	5	1.3 - 2.0	2.9 - 3.5	0.6 - 0.7	1.2 - 1.3	7.0 - 8.4	10.9 - 11.2	4.2 - 4.5	6.1 - 6.2	0.22	0.24	0.41	0.36
Boston Blue Clay	SBC	6	0.5 - 1.0	1.8 - 2.5	0.2 - 0.4	0.7 - 0.9	5.4 - 7.4	9.9 - 10.4	2.9 - 4.0	5.5 - 5.9	0.14	0.24	0.48	0.41
Fargo Clay	SFFC	5	0.1 - 0.3	0.8 - 1.0	0.1	0.3 - 0.4	3.0 - 3.4	6.2 - 6.6	1.7 - 2.1	3.4 - 3.6	0.17	0.24	0.37	0.39
Alaskan Peat	SAP	2	0.7*- 0.9*	1.0 - 1.4	0.3	0.5	6.7*- 7.4*	8.6 - 9.2	4.3*- 4.5*	5.2	0.32*	0.28	0.10*	-0.22
Ice, Artificially Frozen (Horizontal Beams)	SI	6	1.0 - 1.2	1.2 - 1.3	0.4 - 0.5	0.5	9.7 - 10.0	10.1 - 10.4	5.4 - 5.5	5.7 - 5.8	0.29	0.28	0.39	0.34
Ice, Artificially Frozen (Vertical Beams)	SI	4	1.1 - 1.2	1.5 - 1.7	0.4	0.4 - 0.5	9.7 - 10.1	10.4 - 10.6	5.3 - 5.5	5.7 - 5.9	0.36	0.32	0.42	0.38
Ice, Natural - Portage Lake, Maine	SI-(P)	1	1.2*	1.3	0.5*	0.5	- - 10.0*	- - 10.3	5.7*	5.7	0.28*	0.34	0.32*	0.36

(1) The values shown on this table, with the exception of Poisson's ratio, were obtained from the data presented on Figures A1-A14.

(2) Values of Poisson's ratio taken from curves presented in graphs e, Figures A1-A14.

* Extrapolated from graphs.

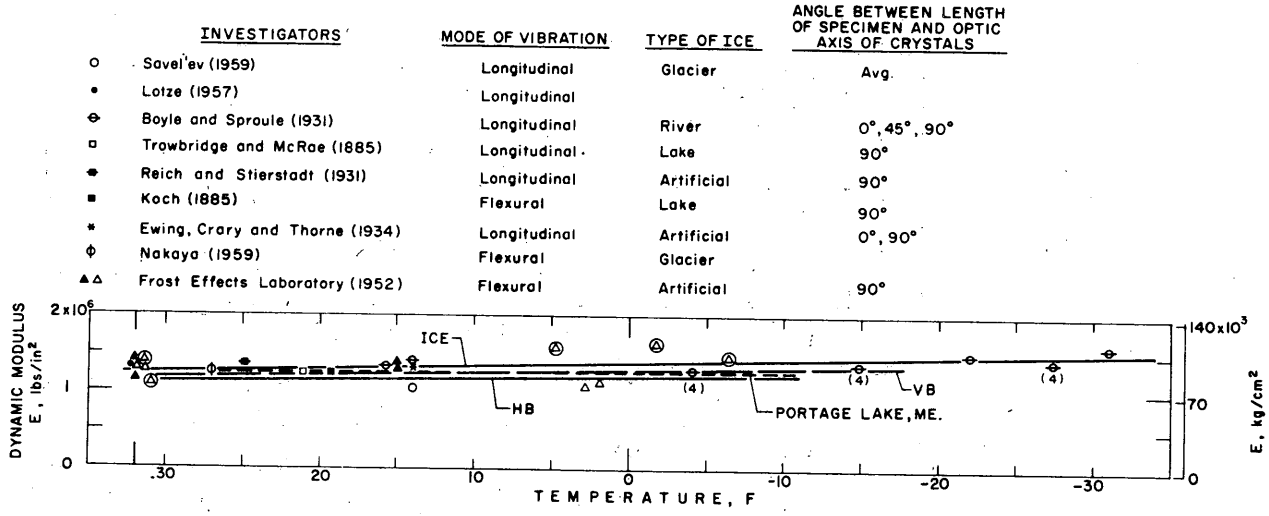

Figure 11. Comparison of dynamic modulus E of ice obtained by various investigators.

For Frost Effects Laboratory tests (1951), circled points indicate flexural vibration parallel to direction of freezing. All other points are for flexural tests in which the vibration was transverse to the direction of freezing. (4) indicates average of four tests by Boyle and Sproule from longitudinal vibrations of rods of river ice. Angles between length of specimens and optic axes of crystals were: 90° in two tests, 45° in one test, and 0° in one test.

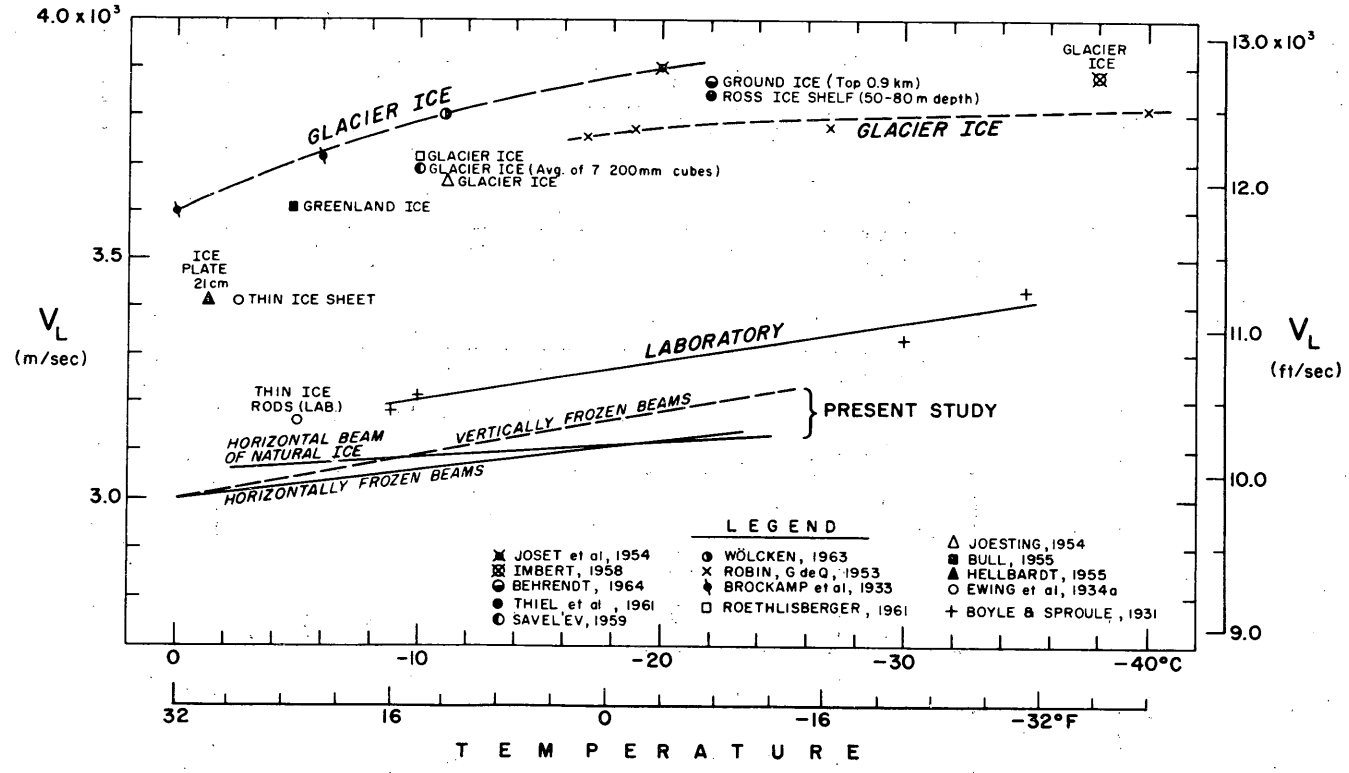

Figure 12. Summary of longitudinal or P-wave velocities in ice measured by various investigators.

Table V. Comparison of propagation velocities of dilatational sonic waves in frozen ground (ft/sec).

Frozen material type	*Investigator*			
	Barnes, 1928	*Joesting, 1954*	*Roethlisberger, 1961*	*Present study*
Sands and gravel	$10.0 - 13.0 \times 10^3$ at 25-30°F	$13.0 - 15.25 \times 10^3$ at 25-30°F	14.7×10^3 at 14°F	$13.6 - 14.1 \times 10^3$ at 25°F
Muck (Silt with organic)		$4.25 - 10.0 \times 10^3$ at 25-30°F		$6.6 - 10.6 \times 10^3$ at 30°F $10.2 - 12.4 \times 10^3$ at -10°F
Glacial till			15.5×10^3 at 13.1°F	$7.2 - 8.0 \times 10^3$ at 30°F $10.6 - 11.9 \times 10^3$ at -10°F

In sharp contrast to the strong temperature dependence of the elastic properties of frozen soils, the elastic properties of ice, whether laboratory frozen or natural, appear little affected by temperature. The elastic wave velocities and elastic moduli for ice, as shown in Figures A12-A14, are only slightly higher at -10F than they are at +30F.

It may also be noted that the dynamic Young's moduli, E, as derived from flexural and longitudinal vibrations differ only slightly, indicating that ice more closely satisfies the assumption of isotropism and homogeneity than frozen soils. This is further indicated by the greater consistency of the test data obtained.

For the soils tested the individual values of dynamic Poisson's ratio, using Young's modulus E determined from longitudinal vibrations, show a wide scattering, ranging roughly from 0.10 to over 0.50 at the higher temperatures, and from approximately 0.15 to 0.45 at -10F. The greater bulk of values fall between 0.25 and 0.40. The silts and clays show greater divergence of values than the soils composed of coarser-grained particles, such as the gravelly sand and the glacial till. The values of Poisson's ratio for ice, although covering a relatively wide range, show the least scattering of all the materials tested.

Some of the wide scatter may be due to the fact that the values of E and G used in computing μ were not measured at exactly the same temperature because of unavoidable operating conditions. Test temperatures may have differed in some cases by as much as 1F.

The wide variation of μ for different specimens of a given soil at a given temperature and mode of vibration also reflects the sensitive dependence of Poisson's ratio upon the values of the modulus of elasticity and rigidity in the formula $\mu = (E/2G) - 1$. A very small percentage change in E and/or G is amplified greatly in the values of μ. For example, assuming $G/E = 0.40$ (a good approximation in most cases): if the error in E and G is only 5% (this is more than a reasonable estimate based upon the scatter of points on the moduli plots), then the maximum error in μ is of the order of 50%. To restrict the maximum error in μ to 20%, E and G must each be determined to an accuracy of the order of 98%, which is very difficult to achieve. In these studies, in view of the many areas of measurement and since E and G are also proportional to the frequency and length squared, it is most probable that the maximum error in any one determination of E and G is unlikely to be less than 5%. For this reason it would appear that any value of Poisson's ratio computed from a single test cannot be considered reliable. Furthermore, the formulae and equations used here are applicable only to homogeneous, isotropic and elastic materials.

Taken as a whole, the values of dynamic Poisson's ratio indicated by the summary curves in Figure 10f and g, which are gased on the average values of the modulus of elasticity derived from flexural and longitudinal vibrations (the average curves in Figure 10c and d) and the values of the modulus of rigidity (the average curves in Figure 10e) appear to be of the right magnitude. However, as stated previously, the flexural values are believed to be somewhat less reliable than the longitudinal values. This evaluation is based largely on the fact that curves of Poisson's ratio vs temperature computed using E from flexural vibrations (Fig. 10f) show a greater variability and inconsistency than those in Figure 10g which were computed using E from longitudinal vibrations. Therefore in subsequent paragraphs, references to and comparison of values of Poisson's ratio will be made only for data plotted in Figure 10g.

From the curves shown in Figure 10f and g it is impossible to express the relationship of Poisson's ratio to temperature in general terms applicable to frozen soils as a whole. Some of the curves are concave in shape, others are convex. For some soils, Poisson's ratio increases with temperature; for others, it decreases.

The greatest variations between μ-values for the different soils occur at the higher temperatures, i.e., above +20F. Whereas the other graphs in Figure 10 reveal an ordered relationship between soil types according to soil texture, and a consistent dependence on temperature, no such relationship is evident for the computed values of μ for these same soils. For example: values of Poisson's ratio (longitudinal) for two clays, Boston blue clay (SBC) and Fargo clay (SFFC), are sharply inconsistent with each other. The μ-values (longitudinal) for two of the silts, Fairbanks silt (SFS) and Yukon silt (SYS), show opposite trends at temperatures below +15F but are reasonably close above that temperature.

The value of Poisson's ratio for ice in the range of -5C to - 15C was determined by Ewing, Crary and Thorne (1934) to be 0.365 ± .007 by use of dynamic methods (longitudinal vibrations); the average curves of Poisson's ratio (longitudinal vibrations) for ice presented in Figures A12e - A14e show comparable values. The individual values, however, ranged from 0.28 to 0.46 in a 40F range, with the greatest differences occurring between specimens frozen vertically. Natural lake ice ranged from 0.32 to 0.36 μ. It is evident here that the same limitation to obtaining a reliable and reproducible value of Poisson's ratio holds for ice as for frozen soils.

The scope of these tests did not include a study of the effect of such factors as crystal size, structure, or specific crystal axis orientation on the elastic properties of ice. However, observations of the general effects of crystal orientation were possible by tests performed on vertically frozen and horizontally frozen ice beams. Crystallography studies of laboratory-frozen ice specimens (Goodby and Kaplar, in prep) reveal that the c-axis is generally oriented parallel to the direction of freezing except near the surface where small crystals have been observed to deviate from the vertical.

The average results from the two different types of beams as shown plotted in Figure 12 show that the longitudinal wave velocities in the vertically frozen beams were slightly higher, the difference in velocity increasing with decreasing temperature. At -20C the difference was about 60 m/sec. Differences of this magnitude were also observed by other investigators (Savel'ev, 1962; Thiel and Ostenso, 1961).

The variations in water content and density occurring in the frozen soils were incidental, resulting from varying degrees of uncontrolled ice segregation which occurred during freezing, and undoubtedly these influenced the elastic behavior. With the limited data available an attempt was made to correlate unit density and water content with the elastic properties but no consistent relationship could be found. A fertile field is present in this area for additional research on frozen soils. Studies of dynamic properties of unfrozen soils (Iida, 1940; Ishimoto *et al.*, 1936; Wilson *et al.*, 1961) show that the dynamic elastic properties of a sand or clay are affected by the unit weight, moisture content, and pressure on the specimen. It is logical to assume that the dynamic elastic

properties of frozen soils would also be dependent upon the unit weight and moisture (ice) content. However, it is not certain whether pressure on saturated frozen soils would have the same influence on unfrozen soil. In unfrozen soil the increase in value of dynamic modulus is believed due to the improved contact of grains under pressure as well as pressure within the grains themselves, but in a saturated frozen soil where the grains are most likely separated by ice the applied pressure may not have the same effect. This is an area where more experimental work is needed. In 1960 the author initiated the development of a triaxial apparatus which will enable lateral and vertical pressures to be applied to a cylindrical soil specimen, which can then be tested for dynamic elastic properties, modulus of elasticity (longitudinal vibration), and the dynamic modulus of rigidity (torsional vibrations) in both the frozen and unfrozen conditions. These two moduli, E and G, will permit the computation of Poisson's ratio, μ, reliable values of which are needed. A contract feasibility study (Foster-Miller Associates, 1960) also indicated the suitability of such an apparatus and technique for measurement of damping coefficients.

A recent increase of interest in the dynamic properties of soils under confining pressures is reflected in the publication of new studies by other investigators (Brutsaert, 1964; Richart, 1960; Wilson *et al.*, 1961). Laboratory studies have been conducted at USA CRREL to determine the elastic properties of soils at various lateral confining pressures using greatly refined techniques and improved apparatus (Stevens, 1964, 1966). These studies were coordinated with field studies, using field vibratory equipment, conducted by the U.S. Army Waterways Experiment Station (Fry, 1963) and the U.S. Army Ohio River Division Laboratory (1964).

A study of graphs a through e on Figure 10 indicates that the elastic properties, the dynamic moduli of elasticity and rigidity, and propagation wave velocities are principally dependent on the type of soil. The coarser-grained soils show higher wave velocities and greater modulus values. The clays have the lowest values, with ice somewhat intermediate. Figure 13, on which the arbitrarily chosen 50% particle size (by weight) has been plotted vs the modulus E_L for 20F, illustrates this relationship more clearly.

The limited data available are not considered sufficient to draw any conclusions as to the effect, if any, of the manner in which the soil specimens were frozen, vertically or horizontally, although one might expect that the orientation of ice lenses in a beam of frozen soil would affect the overall dynamic properties. Additional experimentation with close control of such parameters as soil density and water content might shed more light on the subject. From practical considerations, it would be extremely difficult to arbitrarily control the size and spacing of ice lenses in frost-susceptible soils frozen at normal rates with or without availability of free water.

Suggested further application of dynamic modulus method to study of frozen soil properties. Sonic (dynamic) methods have been used for many years in determining the quality of concrete in slabs and monolithic structures. Kesler and Higuchi (1953) claim to have established a relationship between the dynamic modulus of elasticity, the damping capacity of concrete, and the compressive strength of concrete which enables prediction of the strength of concrete within an error of 5%. Since frozen soils, concrete, and ice are viscoelastic materials, the viscous properties can be evaluated by recording the logarithmic decrement, which is a measure of the damping capacity.

Studies by Chang and Kesler (1956) indicate that there may exist a relationship between the static (creep) and dynamic behavior of concrete. Nakaya (1959) used the dynamic method to study the viscous properties of ice. It would appear that a promising field for further research and study is present to correlate the viscoelastic properties of frozen soils with dynamic properties.

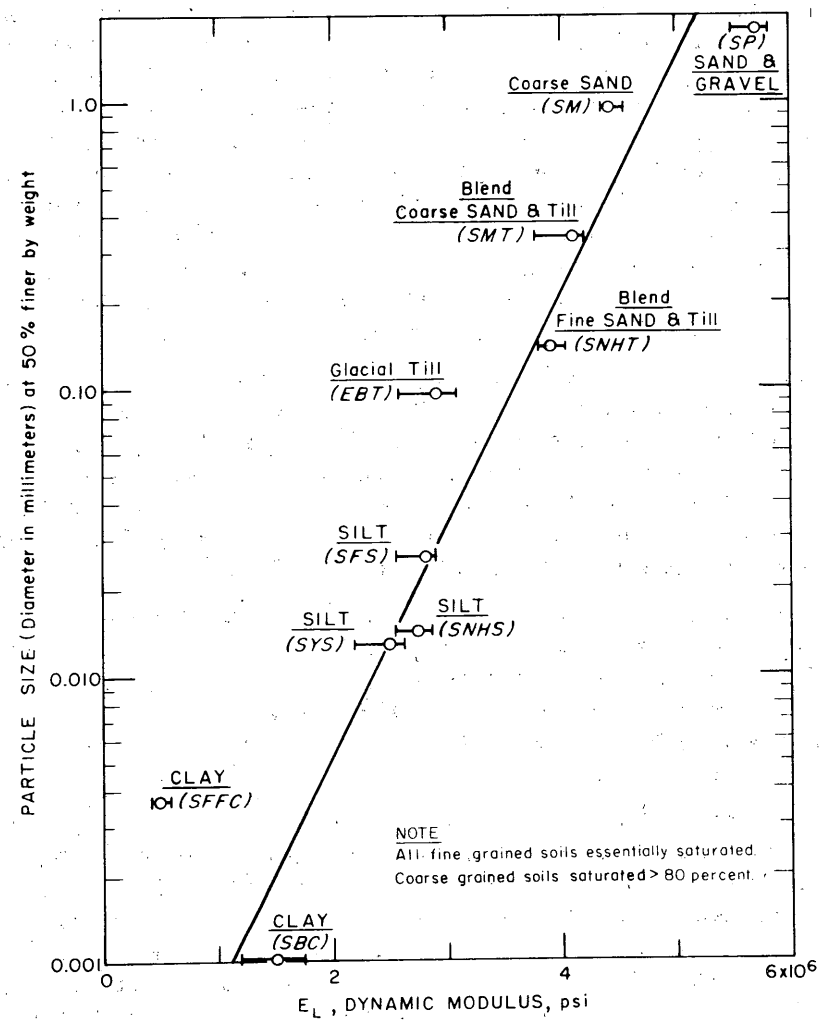

Figure 13. Relationship of soil type and dynamic modulus, E_L, at 20F (-6.7C).

VI. CONCLUSIONS

The following conclusions and observations may be drawn from these and other studies:

1. Vibratory non-destructive techniques can be successfully applied in the laboratory to the study of the dynamic elastic properties of frozen soils and of ice.

2. The technique affords a fertile field for investigation of the viscoelastic properties of frozen soil.

3. The dynamic moduli (E and G) and elastic wave propagation velocities of frozen soils increased with a decrease in temperature: the greatest rate of increase occurred between+20F and +32F. At temperatures lower than +20F the dynamic properties of fine-grained soils (silts and clays) were markedly more temperature-dependent than those of the coarse-grained soils. This dependence is believed chiefly due to the progressive freezing, with decreasing temperature, of additional pore water, both in the adsorbed layer and in the smaller pores, and is a function of grain size. The mineralogical composition of the soil grains and the type and quantity of ions present in the pore water may also be significant contributing factors. Alaskan peat (water content $\sim$300% by weight) and ice showed only a slight increase in modulus and wavetransmission velocities with decreasing temperature.

4. In the range of temperatures used and the degree of saturation achieved in these investigations:

a. The elastic moduli for the coarser-grained soils were more than four times those for fine-grained soils and ice.

b. The wave velocities for coarser-grained soils were more than twice those for the fine-grained soils and ice.

5. Values of Poisson's ratio for frozen soils as computed from average values of E (longitudinal vibrations) and G generally range between $\mu = 0.26$ and 0.38. Within this range average curves of Poisson's ratio vs temperature showed a very irregular, unpredictable pattern unrelated to soil type, although the coarser soils gave more consistent results.

6. The dynamic elastic properties of ice, including elastic wave velocities, as determined by these tests were consistent with findings of other investigators. Values of Poisson's ratio for a given ice specimen showed remarkable consistency throughout the temperature test range although the difference between some specimens was considerable. The average values of Poisson's ratio for the laboratory-frozen ice and natural lake ice, based on results obtained using longitudinal vibrations, ranged from 0.30 to 0.41; but the maximum range of individual values was 0.28 to 0.46.

7. The present limited data are insufficient to draw any conclusions as to the effect, if any, of the manner in which the soil specimens were frozen, i.e., in vertical or horizontal position. However, values of Poisson's ratio computed for individual ice beams frozen vertically show a much greater deviation from the mean than those from horizontally frozen beams, indicating a possible effect of crystal size and structure.

8. All the materials tested were anisotropic and, therefore, high accuracy cannot be expected from the use of simplified theory, assuming isotropy.

9. Velocities and elastic constants developed by procedures such as outlined in this report may be useful in seismic explorations in permafrost and for predicting the response of frozen foundation materials to dynamic loading.

10. The results obtained from these studies pertain to frozen soils which are saturated or close to being saturated.

SELECTED BIBLIOGRAPHY

American Society for Testing and Materials (1962) Symposium on soil dynamics. 64th Annual Meeting, Atlantic City, N.J., June 26, 1961. ASTM Special Technical Publication 305.

_____ (1963) Symposium on dynamic behavior of materials, Albuquerque, N.M., Sept. 27-28, 1962. ASTM Special Technical Publication 336.

Barnes, H.T. (1928) *Ice engineering.* Montreal: Renouf Publishing Company, p. 48-50.

Behrendt, J.C. (1964) Antarctic Peninsula traverse. Geophysical results relating to glaciological and geological studies. The University of Wisconsin, Geophysical and Polar Research Center, Research Report Series No. 64-1.

Bernhard, R.K. (1958) A study of soil wave propagation. *Highway Research Board Proceedings*, vol. 37, p. 618-646.

_____ (1963) Bibliography on soil dynamics. U.S. Army Cold Regions Research and Engineering Laboratory (USA CRREL) Special Report 89.

Boyle, R.W. and Sproule, D.O. (1931) Velocity of longitudinal vibration in solid rods (ultrasonic method) with special reference to the elasticity of ice. *Canadian Journal of Research*, vol. 5, p. 601-618.

Brockamp, B. and Wölcken, K. (1933) The running time curves and ice thickness measurements between West Station and 120 km marginal distance. Wiss. Ergebnisse Deut. Grönland – Expedition Alfred Wegener 1929 und 1930-31, vol. 2. Leipzig: F.A. Brockhaus.

Brutsaert, W. (1964) The propagation of elastic waves in unconsolidated unsaturated granular mediums. *Journal of Geophysical Research,* vol. 69, no. 2.

Bull, C.B.B. (1955) Values of gravity on the inland ice in North Greenland. *Meddelelser om Gronland*, Bd 137, no. 1.

Burmister, D.M. and Stoll, R.D. (1963) Static and dynamic response of granular soils. Columbia University, Department of Civil Engineering and Engineering Mechanics, Technical Report 1 for U.S. Naval Civil Engineering Laboratory, Contract NBy 32198.

Butkovich, T.R. and Landauer, J.K. (1960) Creep of ice at low stress. U.S. Army Snow, Ice and Permafrost Research Establishment (USA SIPRE) Research Report72.

Chang, T.S. and Kesler, C.E. (1956) Correlation of sonic properties of concrete with creep and relaxation. University of Illinois, Department of Theoretical and Applied Mechanics, T and AM Report 94.

Crary, A.P. (1954) Seismic studies on Fletcher's Ice Island, T-3. *Transactions American Geophysical Union*, vol. 35, no. 2, April, p. 293-300.

_____ (1955) Seismic soundings in polar ice. *Geographical Review*, vol. 45, no. 3, July, p. 428-430.

_____; Cotell, R.D.; and Oliver, J. (1952) Geophysical studies in the Beaufort Sea, 1951. *Transactions American Geophysical Union*, vol. 33, April, p. 211-216.

Dorsey, N.E. (1940) *Properties of ordinary water substance.* New York: Reinhold Publishing Corp.

Ewing, M. and Crary, A.P. (1934) Propagation of elastic waves in ice, Part II. *Physics,* vol. 5, p. 181-184.

_____; and Thorne, A.M., Jr. (1934) Propagation of elastic waves in ice, Part I. *Physics,* vol. 5, no. 6, p. 165-168.

Foster-Miller Associates, Inc. (1961) A feasibility study of test method for determining the dynamic properties of soil. Contract Report to U.S. Army Engineer Division, New England.

Fry, Z.B. (1963) Development and evaluation of soil bearing capacity, foundations of structures – field vibratory test data. U.S. Army Engineer Waterways Experiment Station, Technical Report No. 3-632.

Goodby, J.E. and Kaplar, C.W. (in prep.) Ice crystal structure in frozen soils and artificially frozen ice. USA CRREL Research Report 156.

Hardin, B.O. *et al.* (1961) Discussion of paper by F.E. Richart, *Foundation Vibrations*, 1960. *Journal of Soil Mechanics and Foundations Division*, ASCE, Proc. paper 2564.

Hellbardt, G. (1955) Seismische Versuche auf einer Eisplatte (Seismic investigations on an ice plate). *Zeitschrift für Geophysik*, vol. 21, no. 1, p. 41-47.

Hess, H. (1940-41) On the elastic constants of ice. *Zeitschrift für Gletscherkunde*, vol. 27, p. 1-19. USA SIPRE Translation 4, 1950.

Iida, K. (1940) On the elastic properties of soil, particularly in relation to its water content. *Bulletin of the Earthquake Research Institute*, Tokyo Imperial University, vol. 18, p. 675-690.

Imbert, B. (1958) Ice cover and glacial relief. Symposium on Antarctic Research, Wellington, New Zealand (unpublished).

Ishimoto, M. and Iida, K. (1936, 1937) Determination of elastic constants of soils by means of vibration methods: modulus of rigidity and Poisson's ratio. *Bulletin of the Earthquake Research Institute*, Tokyo Imperial University, vol. 14, p. 632-657 (1936) and vol. 15, no. 2, p. 67-85 (1937).

Joesting, H.R. (1954) Geophysical exploration in Alaska. *Arctic*, vol. 7, no. 3 and 4, p. 165-175.

Jones, R. (1958) In-situ measurement of the dynamic properties of soil by vibration methods. *Geotechnique*, vol. VIII, p. 1-21.

Joset, A. and Holtzscherer, J.J. (1954) Expédition Franco-Islandaise au Vatnajökull mars-avril 1951. Resultats des sondages seismiques (French-Icelandic expedition to Vatnajökull in March-April 1951. Results of Seismic Soundings). *Jökull*, vol. 4, p. 1-33 (text in French).

Kaplar, C.W. (1963) Laboratory determination of the dynamic moduli of frozen soils and of ice. *Proceedings: International Conference on Permafrost*, Purdue University.

Kesler, C.E. and Higuchi, Y. (1953) Determination of compressive strength of concrete by using its sonic properties. *Proceedings, American Society for Testing Materials*, vol. 53, p. 1044-1052.

Koch, K.R.(1885) Beiträge zur Kenntniss der Elasticität des Eises (The elasticity of ice). *Annalen der Physik*, 3rd Ser, vol. 25,p.438-450.

Kornfeld, M. and Shestikhin, P. (1942) Elasticity of a crystal as dependent on temperature. Comptes Rendus Akad Nauk SSSR, vol. 36, no. 2, p. 52-56.

Lagutin, B.L. and Shul'man, A.P. (1946) "O metodakh roscheta ledianykh perepray" ("Methods of calculating the load carrying capacity of ice crossings") in *Data on the problem of ice crossings*. Trudy Nauchno-Issledovatel'skikh Uchrezhdeniya Seriya 5, Vyp. 20, Glavneye Upravleniye Gidrometeorologicheskoy Sluzhly Gidrometeoizdat Sverdlovsk, Moscow. U.S. Army Corps of Engineers, New England Division, ACFEL Translation 25, 1954, p. 46-63.

Lane, K.S. (1948) Providence vibrated density test. *Proceedings of the Second International Conference on Soil Mechanics and Foundation Engineering*, vol. 4, p. 243-.

Lawrence, F.V. (1961) Response of soils to dynamic loadings, Report 8: Laboratory measurement of dilatational wave propagation velocity. U.S. Army Corps of Engineers, Waterways Experiment Station.

Leet, L.D. (1950) Earth waves. Cambridge, Mass.: Harvard University Press; Harvard Monographs in Applied Science, no. 2.

Lotze, W. (1957) Sound velocity measurements on ice as dependent on pressure and temperature. *Zeitschrift für Geophysik*, vol. 23, no. 5, p. 242-249.

Love, A.E.H. (1892) *A treatise on the mathematical theory of elasticity*. Cambridge: University Press, 4th edition, 1927.

Mason, W.P.(1935) Motion of a bar vibrating in flexure, including the effect of rotary and lateral inertia. *Journal of the Acoustical Society of America*, vol. 6, p. 246.

Nakaya, U. (1959) Visco-elastic properties of snow and ice in the Greenland Ice Cap. USA SIPRE Research Report 46.

Northwood, T.D. (1947) Sonic determination of the elastic properties of ice. *Canadian Journal of Research*, vol. 25, p. 88-95.

Obert, L. and Duval, W.I. (1939) Sonic method of determining the modulus of elasticity of building materials under pressure. *Proceedings, American Society for Testing Materials*, vol. 39, p. 987.

Oliver, J.; Crary, A.P.; and Cotell, R.D. (1954) Elastic waves in arctic pack ice. *Transactions American Geophysical Union*, vol. 35, p. 282-292.

Pickett, G. (1945) Equations for computing elastic constants from flexural and torsional resonant frequencies of vibration of prisms and cylinders. *Proceedings, American Society for Testing Materials*, vol. 45, p. 846-865.

Press, F. *et al.* (1951) Air-coupled flexural waves in floating ice. *Transactions American Geophysical Union*, vol. 32, April, p. 166-172.

Quinlan, P.M. (1953) The elastic theory of soil dynamics. Symposium on Dynamic Testing of Soils, ASTM STP no. 156, p. 3-33.

Rayleigh (Lord) (1929) *Theory of sound.* New York: McMillan Publishing Co., p. 250.

Richart, F.E., Jr. (1960) Foundation vibrations. *Journal of the Soil Mechanics and Foundations Division*, ASCE, Proc. paper 2564.

_____; Hall, J.R., Jr.; and Lysmer, J. (1962) Study of the propagation and dissipation of elastic wave energy in granular soils. University of Florida for U.S. Army Corps of Engineers, Waterways Experiment Station. Contract DA-22-079-ENG-314.

Robin, G. deQ. (1953) Measurements of ice thickness in Dronning Maud Land, Antarctica. *Nature*, vol. 171, January, p. 55-58.

Roethlisberger, H. (1961) The applicability of seismic refraction soundings in permafrost near Thule, Greenland. USA CRREL Technical Report 81.

Savel'ev, B.A. (1962) "Gliatsiologicheskie issledovania Chetvertoi Antarkticheskoi Ekspeditsii (1959)" ("Glaciological investigations of the Fourth Antarctic Expedition (1959)") in *Materials of glaciological investigations: Chronicle and discussions.* Institute Geografii AN SSSR, Issue4, p. 54-57 (text in Russian).

Stevens, H.W. (1964) Results of tests for properties of sand specimens under dynamic loads (Biloxi sand). USA CRREL Technical Note (unpublished).

_____ (1966) Measurement of the complex moduli and damping of soils under dynamic loads. USA CRREL Technical Report 173.

Swain, R.J. (1962) Recent techniques for determination of "in-situ" elastic properties and measurement of motion amplification in layered media. *Geophysics*, vol. 27, no. 2, p. 237-241.

Swift, H.W. (1926) Determination of the modulus of elasticity by dynamical methods. *Philosophical Magazine*, Series7, vol. 2, no. 8, p. 351-368.

Tabata, T. (1958) Kaihyo no rikigakuteki seishitsu no kenkyu. III. Shindoho ni yoru tanseiritsu no sokutei (2) (Studies on mechanical properties of sea ice. III. Measurement of elastic modulus by the lateral vibration method (2)). *Teion-kagaku* (Low *Temperature Science*, Ser. A, vol. 18, p. 116-129.

Thiel, E. and Ostenso, N.A. (1961) Seismic studies on Antarctic ice shelves. *Geophysics*, vol. XXVI, no. 6, p. 706-715.

Trowbridge, J. and McRae, A.L. (1885) Elasticity of ice. *American Journal of Science*, 3rd Ser., vol. 129, p. 349-355.

Tsytovich, N.A. (1940) An investigation of the elastic and plastic deformation of frozen ground. Trans. Akad Nauk SSSR, vol. 10, p. 5-36.

_____ (1957) The fundamentals of frozen ground mechanics (New investigations). 4th International Conference on Soil Mechanics and Foundation Engineering, p. 116.

Tsytovich, N.A. and Sumgin, M.I. (1937) "Deformation of frozen ground under vertical load" in *Osnovaniia mekhaniki merzlykh gruntov (The principles of mechanics of frozen ground).* Moscow: Izdatel'stvo Akad Nauk SSSR, Chap. 5. USA SIPRE Translation 19, Chap. 5, 1959.

_____ and Vologdina, I.S. (1936) Determination of elastic constants of frozen grounds and examination of their properties of plasticity. Trans. Akad Nauk SSSR, vol. 3, p. 7-54.

U.S. Army Arctic Construction and Frost Effects Laboratory (1952) Investigation of description, classification and strength properties of frozen soils, Fiscal Year 1951. U.S. Army Corps of Engineers, New England Division, ACFEL Technical Report 40; USA SIPRE Report 8.

_____ (1953) Investigation of the strength properties of frozen soils, Fiscal Year 1952. U.S. Army Corps of Engineers, New England Division, ACFEL Technical Report 44.

_____ (1954) Investigation of the strength properties of frozen soils, Fiscal Year 1953. U.S. Army Corps of Engineers, New England Division, ACFEL Technical Report 48.

U.S. Army Ohio River Division Laboratory (1964) Radar tower foundation design. Control of tilting for wind loadings. U.S.Army Corps of Engineers, EC-1110-345-147, Circular no. 1110-345-147.

Wilson, J.T. and Strong, R. (1948) Bibliography on lake ice. University of Michigan, Engineering Research Institute, 87 p.

Wilson, S.D. and Miller, R.P. (1961) Discussion of the paper by Richart (1960). *Journal of the Soil Mechanics and Foundations Division,* ASCE, April, p. 164-169.

_____ and Dietrich, R.J. (1961) Effect of consolidation pressure on elastic and strength properties of clay. *Proceedings, ASCE Research Conference on Shear Strength of Cohesive Soils,* Boulder, Colorado, June, 1961.

Wölcken, K.(1961) Seismic ice-thickness measurements on Novaya Zemlya, 1932-33. *Polarforschung*, vol. 5 (½), p. 87-91.

TABLE AI

TABULATION OF THE MEASURED FUNDAMENTAL RESONANT FREQUENCIES FOR DYNAMIC MODULUS TESTS

Specimen No.	Flexural		Longitudinal		Torsional	
	Temp. °F.	Freq. cps	Temp. °F.	Freq. cps	Temp. °F.	Freq. cps
SP-300 (Horizontal Beam)	30.0	1626	29.2	6530	29.6	3690
	24.9	1728	24.2	6820	24.5	3920
	20.3	1734	19.6	6908	19.9	3970
	9.9	1745	9.0	7110	9.5	4055
	2.7	1782	0.4	7050	1.0	4063
	-14.3	1782	-16.5	7210	-15.7	4129
	-17.0	1850	-18.5	7253	-18.0	4160
SP-301 (Horizontal Beam)	29.9	1638	28.7	6800	28.8	3960
	25.2	1775	24.7	7020	25.0	4096
	19.8	1792	19.1	7142	19.4	4140
	10.7	1825	10.0	7310	10.3	4190
	1.5	1830	-0.2	7332	0.6	4200
	-13.0	1837	-13.8	7367	-13.7	4242
	-16.0	1862	-17.0	7422	-16.7	4295
SM-154 * (Horizontal Beam)	29.8	1440	29.8	5890	29.8	3640
	21.0	1520			21.0	3690
	14.0	1550	14.0	6350	14.0	3770
	2.0	1569	2.0	6400	2.0	3800
	-11.0	1569	-14.0	6550	-13.0	3850
SM-200 (Vertical Beam)	31.4	1471	30.1	5559	28.8	3270
	23.3	1521	23.4	6200	23.5	3530
	11.5	1558	10.5	6400	9.5	3680
	1.0	1608	0.0	6500	-2.0	3690
	-8.7	1615	-9.0	6900	-8.0	3740
SMT-306 (Vertical Beam)	30.1	1243	30.0	4664	29.9	2623
	25.8	1539	25.6	5759	25.7	3230
	22.1	1639	21.4	6100	21.8	3450
	17.7	1696	17.4	6300	17.5	3580
	8.6	1763	7.9	6510	8.0	3640
	-0.6	1827	-1.5	6610	-1.1	3760
	-9.7	1893	-10.3	6800	-10.2	3930
SMT-307 (Vertical Beam)	30.6	1100	30.5	4633	30.5	2500
	26.1	1470	25.5	5811	25.7	3340
	22.4	1549	21.6	6220	21.8	3550
	17.1	1629	16.6	6380	16.9	3680
	7.2	1706	6.1	6650	6.5	3860
	-0.8	1795	-2.0	6800	-1.6	3970
	-10.2	1911	-11.2	6920	-10.9	4077
SMT-308 (Vertical Beam)	30.7	1110	30.7	4581	30.6	2421
	26.5	1439	26.2	5782	26.3	3270
	22.3	1569	21.5	6230	21.9	3480
	17.8	1639	17.5	6410	17.6	3670
	7.8	1708	7.1	6740	7.4	3880
	-0.8	1806	-1.7	6910	-1.3	3940
	-9.7	1920	-10.5	7100	-10.3	4014
SMT-309 (Vertical Beam)	30.4	1049	30.2	4633	30.3	2511
	25.9	1459	25.5	5781	25.6	3300
	22.9	1549	22.5	6120	22.6	3480
	17.2	1647	16.7	6320	17.0	3660
	8.4	1719	7.8	6720	8.1	3870
	0.2	1792	-0.9	6900	-0.3	4043
	-10.2	1831	-11.4	7010	-10.8	4073
SMT-310 (Vertical Beam)	30.0	1273	30.0	4873	30.1	2623
	26.5	1619	26.4	5734	26.5	3300
	22.1	1773	20.9	6320	21.5	3620
	17.9	1863	17.5	6500	17.6	3750
	8.7	1920	8.1	6730	8.2	3820
	-0.3	2000	-1.7	6920	-1.1	3860
	-9.1	2045	-10.2	7111	-9.8	4030
SNHT-306 (Vertical Beam)	24.6	1646	23.5	6170	23.9	3545
	20.0	1707	19.8	6300	19.7	3660
	11.7	1783	10.4	6590	10.8	3840
	-0.4	1797	-0.9	6600	-0.7	3900
	-8.5	1850	-9.1	6890	-8.9	3990
SNHT-307 (Vertical Beam)	26.4	1549	25.3	6100	25.6	3480
	20.7	1637	20.0	6300	20.3	3680
	13.0	1734	12.1	6530	12.4	3840
	2.0	1783	1.1	6730	1.4	3960
	-7.7	1812	-8.5	6840	-8.2	4023
SNHT-308 (Vertical Beam)	25.8	1558	25.0	6120	25.3	3470
	20.0	1655	20.0	6320	19.9	3635
	12.1	1723	10.4	6600	10.9	3820
	2.0	1793	0.9	6730	1.3	3890
	-7.6	1835	-8.0	6900	-7.9	3980
SNHT-309 (Vertical Beam)	27.0	1558	26.2	6100	26.4	3430
	19.8	1684	19.1	6400	19.4	3670
	11.9	1734	11.0	6630	11.3	3880
	0.7	1804	-0.7	6820	-0.2	4000
	-8.7	1813	-9.0	6900	-9.2	4044
SNHT-310 (Vertical Beam)	25.3	1593	23.9	6130	24.3	3625
	17.6	1707	15.7	6400	16.3	3870
	13.5	1743	12.8	6530	13.1	3910
	3.3	1832	1.8	6750	2.1	3980
	-9.0	1885	-10.0	6850	-9.7	4011
SEBT-304 (Vertical Beam)	24.8	1228	24.2	4813	24.3	2748
	19.8	1317	20.7	5146	19.7	2930
	9.5	1491	8.9	5869	9.1	3320
	0.9	1533	-0.4	6030	0.1	3460
	-11.7	1638	-13.1	6220	-12.6	3580
SEBT-305 (Vertical Beam)	24.9	1191	24.5	4612	24.6	2720
	22.4	1305	21.5	5337	21.8	2980
	9.5	1510	8.9	5869	9.1	3345
	2.0	1588	1.1	6210	1.3	3510
	-8.8	1638	-9.6	6350	-9.4	3690
SEBT-306 (Vertical Beam)	24.6	1203	24.3	5078	24.4	2828
	20.1	1347	19.6	5359	19.6	3070
	10.1	1460	9.6	5890	9.7	3410
	0.8	1539	0.0	6200	0.1	3560
	-9.5	1594	-10.2	6400	-10.0	3670
SEBT-307 (Vertical Beam)	24.2	1202	23.1	4789	23.5	2757
	22.3	1243	21.5	5059	21.8	2827
	8.9	1449	7.1	5659	8.2	3240
	2.2	1520	1.9	5891	1.7	3380
	-9.2	1549	-10.2	6200	-9.9	3470
SEBT-308 (Vertical Beam)	24.9	1337	24.5	4637	24.6	2889
	19.5	1480	19.0	5358	19.2	3140
	7.4	1603	6.0	5901	6.4	3430
	3.1	1674	2.4	6140	2.8	3540
	-10.0	1738	-11.0	6300	-10.7	3680
SNHS-150 (Vertical Beam)	30.3	1242	29.5	5114	29.0	2683
	17.7	1334	17.5	5335	16.5	3180
	9.5	1396	8.5	5391	8.0	3220
	-0.5	1408	-1.0	5444	-1.5	3330
	-7.0	1439	-8.0	5444	-7.0	3340
SNHS 152 * (Horizontal Beam)	29.0	1334	30.0	5335	31.0	2290
	20.5	1418	20.5	5400	20.5	3030
	10.5	1405	11.0	5600	11.0	3110
	3.2	1500	2.0	5670	2.0	3250
	-6.0	1550	-6.0	5723	-6.0	5250
SNHS 153 * (Horizontal Beam)	29.0	1332	29.0	4966	29.0	2910
	17.0	1470	17.0	5035	17.0	3050
	9.0	1510	9.0	5535	9.0	3290
	-3.0	1556	-3.0	5670	-3.0	3370
	-15.0	1510	-15.0	5890	-15.0	3400

NOTE: Physical data on specimens are given in Table III.

TABLE AI (CONT'D)

TABULATION OF THE MEASURED FUNDAMENTAL RESONANT FREQUENCIES FOR DYNAMIC MODULUS TESTS

Specimen No.	Flexural		Longitudinal		Torsional	
	Temp. °F.	Freq. cps	Temp. °F.	Freq. cps	Temp. °F.	Freq. cps
SFS-374 (Vertical Beam)	31.1	1090	30.8	4581	30.4	2421
	28.3	1306	28.2	4990	27.8	2795
	24.3	1420	23.6	5279	23.8	2929
	22.0	1490	20.7	5529	21.0	3080
	12.3	1561	11.5	5713	11.5	3280
	5.3	1591	4.2	5833	4.7	3440
	-2.3	1621	-3.5	5922	-2.9	3470
	-9.0	1646	-7.9	6000	-8.7	3580
SFS-375 (Vertical Beam)	30.4	1038	30.1	4056	30.1	2490
	28.2	1242	27.6	4687	27.8	2782
	24.5	1350	24.2	4928	24.3	3080
	21.5	1445	20.7	5568	21.1	3230
	13.4	1524	11.2	5736	13.0	3384
	6.0	1568	5.2	5834	5.4	3510
	-2.3	1593	-3.5	6010	-2.9	3570
	-8.8	1602	-9.6	6100	-9.1	3590
SFS-376 (Vertical Beam)	31.0	1038	30.5	4319	30.9	2291
	28.3	1212	28.3	4633	28.2	2839
	23.9	1398	23.0	5000	23.4	3070
	22.5	1420	21.5	5560	21.8	3190
	11.4	1557	10.6	5801	11.0	3450
	4.8	1581	4.2	5980	4.6	3490
	-2.3	1616	-2.9	6120	-2.7	3565
	-8.5	1621	-10.0	6150	-9.2	3610
SFS-377 (Vertical Beam)	31.8	1069	31.0	4160	31.2	2091
	27.5	1294	27.1	5110	26.9	2746
	24.5	1388	23.4	5248	23.6	2925
	21.9	1429	21.6	5560	22.0	3140
	14.0	1543	12.4	5790	13.5	3280
	5.1	1574	3.4	5890	4.3	3435
	-3.2	1610	-4.3	6110	-4.0	3480
	-7.8	1626	-9.4	6300	-8.0	3560
SFS-378 (Vertical Beam)	30.7	1130	30.4	4160	30.5	2391
	27.9	1347	27.7	5012	27.6	2828
	24.2	1499	23.6	5258	23.7	3020
	21.5	1549	20.7	5680	20.9	3140
	11.4	1651	10.8	5847	10.9	3370
	4.4	1676	3.4	5890	3.8	3450
	-3.1	1686	-3.8	6090	-3.3	3560
	-5.4	1696	-6.2	6110	-6.0	3660
SYS-376 (Vertical Beam)	30.0	1079	29.8	4317	29.9	2312
	26.0	1049	25.8	4517	25.8	2461
	21.1	1286	20.4	5000	20.6	2809
	15.6	1408	14.7	5334	14.9	2920
	6.8	1524	5.9	5618	6.1	3100
	-1.6	1534	-3.1	5781	-2.7	3230
	-10.7	1558	-11.3	5924	-11.5	3330
SYS-377 (Vertical Beam)	29.9	1120	29.4	4161	29.6	2292
	26.3	1091	25.6	4266	25.7	2431
	25.2	1130	24.6	4318	24.8	2452
	21.0	1100	20.4	5090	20.6	2728
	16.2	1228	14.6	5279	15.6	2950
	7.6	1306	6.4	5590	6.8	3080
	-1.0	1389	-2.0	5690	-1.6	3250
	-11.3	1444	-12.8	5891	-12.3	3350
SYS-378 (Vertical Beam)	30.0	1059	29.5	4474	29.9	2382
	24.9	1091	24.4	4528	24.6	2594
	21.3	1243	20.7	4995	20.9	2757
	16.6	1343	15.1	5224	15.8	2941
	7.2	1423	6.4	5545	6.7	3080
	0.3	1449	-1.3	5758	-0.5	3280
	-12.2	1549	-13.4	5891	-13.0	3390

Specimen No.	Flexural		Longitudinal		Torsional	
	Temp. °F.	Freq. cps	Temp. °F.	Freq. cps	Temp. °F.	Freq. cps
SYS-379 (Vertical Beam)	30.4	1106	30.0	4453	30.1	2412
	25.1	1112	24.6	4687	24.7	2500
	20.7	1233	20.1	5189	20.2	2819
	14.9	1300	14.4	5447	14.5	3030
	7.1	1411	5.8	5680	6.0	3150
	-0.6	1499	-1.7	5781	-1.5	3230
	-9.5	1554	-10.1	5924	-10.0	3310
SYS-380 (Vertical Beam)	30.6	1120	30.4	4264	30.5	2402
	25.7	1296	24.8	4769	25.0	2695
	20.7	1428	19.8	5338	20.1	2960
	13.6	1549	12.0	5569	12.7	3150
	7.2	1593	6.1	5691	6.4	3200
	0.6	1676	0.3	5781	0.4	3280
	-9.5	1725	-11.7	6120	-10.3	3760
SBC-307 (Horizontal Beam)	29.1	781	28.8	3230	28.9	1714
	24.7	979	24.3	4000	24.4	2161
	19.8	1041	19.2	4473	19.4	2391
	9.3	1202	8.0	4894	8.3	2674
	-1.6	1296	-3.1	5278	-2.7	2930
	-7.0	1376	-8.7	5358	-8.4	3010
SBC-307A (Horizontal Beam)	30.3	666	30.2	2910	30.2	1637
	25.0	970	24.3	3970	24.5	2172
	19.5	1090	18.7	4498	18.9	2471
	9.1	1255	7.9	5144	8.3	2865
	-2.7	1398	-3.8	5469	-3.5	3040
	-8.7	1429	-10.5	5702	-9.9	3130
SBC-308 (Horizontal Beam)	-	-	25.3	3880	-	-
	19.9	1111	19.2	4476	19.5	2561
	10.5	1262	9.2	5000	10.0	2746
	0.0	1337	-1.5	5224	-1.0	2945
	-8.7	1408	-10.4	5436	-9.7	3020
SBC-309 (Horizontal Beam)	30.3	863	29.9	3570	30.1	1910
	25.9	1105	25.3	4370	25.4	2361
	19.2	1238	18.3	4790	18.7	2697
	9.3	1365	8.5	5333	8.7	2920
	-0.6	1438	-2.1	5623	-1.5	3090
	-9.5	1520	-10.7	5781	-10.2	3255
SBC-309A (Horizontal Beam)	31.9	852	31.7	3670	31.5	1980
	25.5	1191	24.4	4739	24.6	2697
	19.2	1252	17.1	5123	17.4	2839
	8.1	1346	7.1	5448	7.5	3060
	-1.8	1389	-3.2	5612	-2.9	3150
	-7.5	1470	-9.4	5769	-8.5	3200
SBC-310 (Horizontal Beam)	30.0	739	29.6	3360	30.0	1764
	24.5	1020	23.8	4264	24.0	2271
	21.0	1040	19.9	4487	20.2	2481
	8.8	1293	7.3	5045	7.9	2869
	-1.1	1382	-2.5	5447	-1.9	3010
	-9.1	1448	-10.7	5758	-10.2	3090
SFFC-366 (Horizontal Beam)	30.1	382	29.7	1851	29.9	1111
	25.4	510	24.9	2222	25.1	1212
	21.9	610	21.5	2648	21.5	1419
	10.0	667	9.7	2849	9.7	1550
	-2.5	752	-3.2	3170	-3.0	1598
	-7.8	822	-9.5	3350	-9.0	1909
SFFC-366A (Horizontal Beam)	30.0	391	29.5	1840	29.7	1151
	26.6	489	25.7	2213	26.2	1202
	20.0	573	19.2	2543	19.4	1470
	10.6	651	10.5	2870	10.2	1540
	-3.2	750	-6.6	3380	-4.0	1793
	-7.8	771	-9.2	3630	-8.7	2122

TABLE AI (CONT'D)

TABULATION OF THE MEASURED FUNDAMENTAL RESONANT FREQUENCIES FOR DYNAMIC MODULUS TESTS

Specimen No.	Flexural		Longitudinal		Torsional	
	Temp. °F.	Freq. cps	Temp. °F.	Freq. cps	Temp. °F.	Freq. cps
SFFC-367 (Horizontal Beam)	30.4	364	29.4	1734	29.4	1010
	24.7	469	24.3	2221	24.5	1283
	19.9	531	19.6	2614	19.9	1428
	-11.0	609	10.6	2848	10.7	1539
	-1.4	699	-2.4	3250	-2.2	1792
	-6.7	771	-8.3	3280	-7.2	2171
SFFC-368 (Horizontal Beam)	30.8	341	30.5	1588	30.5	874
	26.9	470	26.2	2091	26.3	1140
	19.1	578	17.8	2542	18.1	1439
	12.3	650	11.9	2778	12.0	1578
	-2.6	765	-3.5	3190	-3.3	1782
	-7.8	822	-9.3	3280	-8.2	1782
SFFC-369 (Horizontal Beam)	31.4	351	30.9	1618	31.1	831
	26.5	460	25.7	2102	25.9	1130
	21.2	561	20.5	2634	20.8	1377
	6.5	733	8.0	2859	8.1	1589
	-3.0	753	-4.8	3240	-3.7	1762
	6.3	831	-7.1	3330	-6.7	1811
SAP-148 (Vertical Beam)	29.4	1082	29.0	3870	28.3	2380
	20.5	1112	20.6	4160	20.8	2360
	6.3	1143	6.4	4370	6.5	2560
	-1.5	1194	-2.5	4685	-3.5	2680
	-12.0	1235	-12.0	4475	-12.0	2710
SAP-150 (Horizontal Beam)	26.9	831	26.9	3450	26.9	2191
	22.0	913	22.0	3750	22.0	2233
	13.0	980	13.0	4055	13.0	2360
	2.0	1000	2.0	4368	2.0	2452
	-8.0	1049	-10.0	4474	-8.0	2540
SI-664 (Vertical Beam)	27.6	1407	26.4	5480	26.0	3000
	22.6	1425	22.0	5545	21.4	3010
	19.8	1435	17.4	5557	18.6	3030
	13.2	1445	12.4	5579	11.5	3040
	9.7	1460	8.8	5645	8.8	3070
	3.1	1470	1.6	5668	0.5	3110
	-3.5	1480	-2.5	5755	-4.2	3130
	-7.5	1500	-8.5	5783	-8.0	3150
	-12.3	1510	-13.9	5858	-13.3	3170
SI-665 (Vertical Beam)	28.8	1425	28.3	5334	27.9	3060
	26.0	1435	25.4	5351	24.8	3070
	21.0	1440	20.2	5368	20.4	3080
	14.0	1450	13.4	5435	13.0	3100
	7.7	1480	7.2	5569	6.8	3180
	3.0	1515	2.4	5623	2.4	3220
	-5.0	1521	-5.5	5657	-5.5	3240
	-7.5	1529	-8.0	5670	-8.9	3270
	-12.5	1548	-13.8	5747	-13.1	3280
SI-667 (Vertical Beam)	29.6	1480	29.9	5445	30.1	2955
	26.8	1495	25.4	5533	24.9	2980
	22.2	1500	20.8	5569	20.2	3005
	15.1	1520	16.1	5635	15.4	3030
	9.7	1525	8.9	5669	8.4	3080
	2.6	1530	0.4	5679	1.2	3100
	-6.0	1540	-8.9	5770	-7.5	3150
	-7.7	1549	-9.5	5782	-8.5	3170
	-11.6	1578	-13.0	5835	-12.3	3185

Specimen No.	Flexural		Longitudinal		Torsional	
	Temp. °F.	Freq. cps	Temp. °F.	Freq. cps	Temp. °F.	Freq. cps
SI-668 (Vertical Beam)	27.7	1419	27.5	5436	27.0	3040
	23.8	1429	23.5	5467	23.2	3050
	21.5	1440	20.6	5540	19.6	3080
	15.6	1470	15.5	5550	15.3	3130
	11.4	1485	10.1	5590	9.5	3180
	4.7	1515	3.5	5680	3.5	3210
	-5.0	1529	-6.5	5735	-8.5	3260
	-8.0	1529	-9.8	5758	-10.5	3270
	-12.8	1534	-14.7	5780	-14.0	3280
SI-670 (Horizontal Beam)	28.3	1418	28.0	5457	28.0	2980
	26.1	1418	25.9	5480	25.9	2990
	21.2	1434	20.8	5534	21.1	3040
	12.6	1449	12.2	5560	12.6	3070
	1.5	1469	0.0	5579	0.8	3110
	-8.5	1515	-8.7	5669	-8.7	3150
SI-671 (Horizontal Beam)	31.6	1397	31.5	5418	31.3	3015
	28.6	1409	28.6	5423	28.5	3020
	25.6	1414	25.8	5448	25.6	3035
	20.2	1424	19.8	5480	20.0	3070
	12.8	1439	12.9	5546	12.9	3140
	1.5	1460	0.4	5579	1.0	3155
	-9.8	1480	-10.2	5624	-10.0	3170
SI-672 (Horizontal Beam)	28.6	1397	28.6	5423	28.6	3040
	25.4	1414	25.3	5457	25.4	3045
	20.0	1424	19.4	5511	19.6	3060
	12.3	1439	12.3	5551	12.0	3115
	3.8	1454	2.5	5584	3.0	3130
	-7.0	1480	-6.3	5624	-6.2	3180
SI-673 (Horizontal Beam)	28.9	1360	28.9	5407	29.0	2990
	25.1	1368	25.2	5435	25.2	3010
	21.5	1371	21.4	5468	21.4	3050
	10.4	1403	10.3	5534	10.2	3095
	2.9	1418	3.0	5559	3.1	3130
	-7.6	1434	-8.7	5646	-7.8	3220
SI-674 (Horizontal Beam)	31.0	1339	30.8	5329	30.7	3010
	28.4	1346	28.1	5340	28.0	3015
	26.4	1346	26.1	5357	26.2	3025
	21.5	1368	21.0	5423	21.2	3045
	9.4	1388	8.5	5457	9.0	3070
	3.3	1409	1.7	5511	2.5	3120
	-10.2	1431	-10.6	5559	-10.9	3150
SI-675 (Horizontal Beam)	28.4	1393	28.0	5435	28.1	3000
	24.4	1403	23.7	5468	23.8	3020
	20.7	1414	20.2	5511	20.2	3075
	11.1	1434	10.2	5559	10.5	3110
	3.8	1449	2.7	5613	3.2	3120
	-10.3	1469	-10.2	5655	-10.2	3143
SI-(P)** (Horizontal Beam)	27.7	1582	27.5	5781	27.2	3280
	25.0	1593	25.0	5781	25.0	3280
	20.5	1593	20.2	5789	20.2	3285
	12.7	1608	12.0	5833	12.3	3290
	5.7	1612	5.9	5853	5.4	3290
	-6.6	1621	-7.2	5890	-7.2	3300

NOTES: Vertical beams were frozen in vertical position from top to bottom - ice lenses in soil specimens oriented normal to longitudinal axis of beam.

Horizontal beams were frozen in horizontal position from top to bottom - ice lenses in soil specimens oriented parallel to longitudinal axis of beam.

ALNICO bar magnets used with all test specimens, except those marked with asterisk (*). Dimensions of bar magnets: 3/16 x 3/16 x 2 inches. Weight: 16 grams per pair.

* ALNICO cylindrical magnets used with these specimens. Dimensions of cylindrical magnets: 3/16-inch diameter x 1.8 inches. Weight: 12 grams per pair.

** Specimen was cut from naturally frozen lake ice from Portage Lake, Maine, in March 1953.

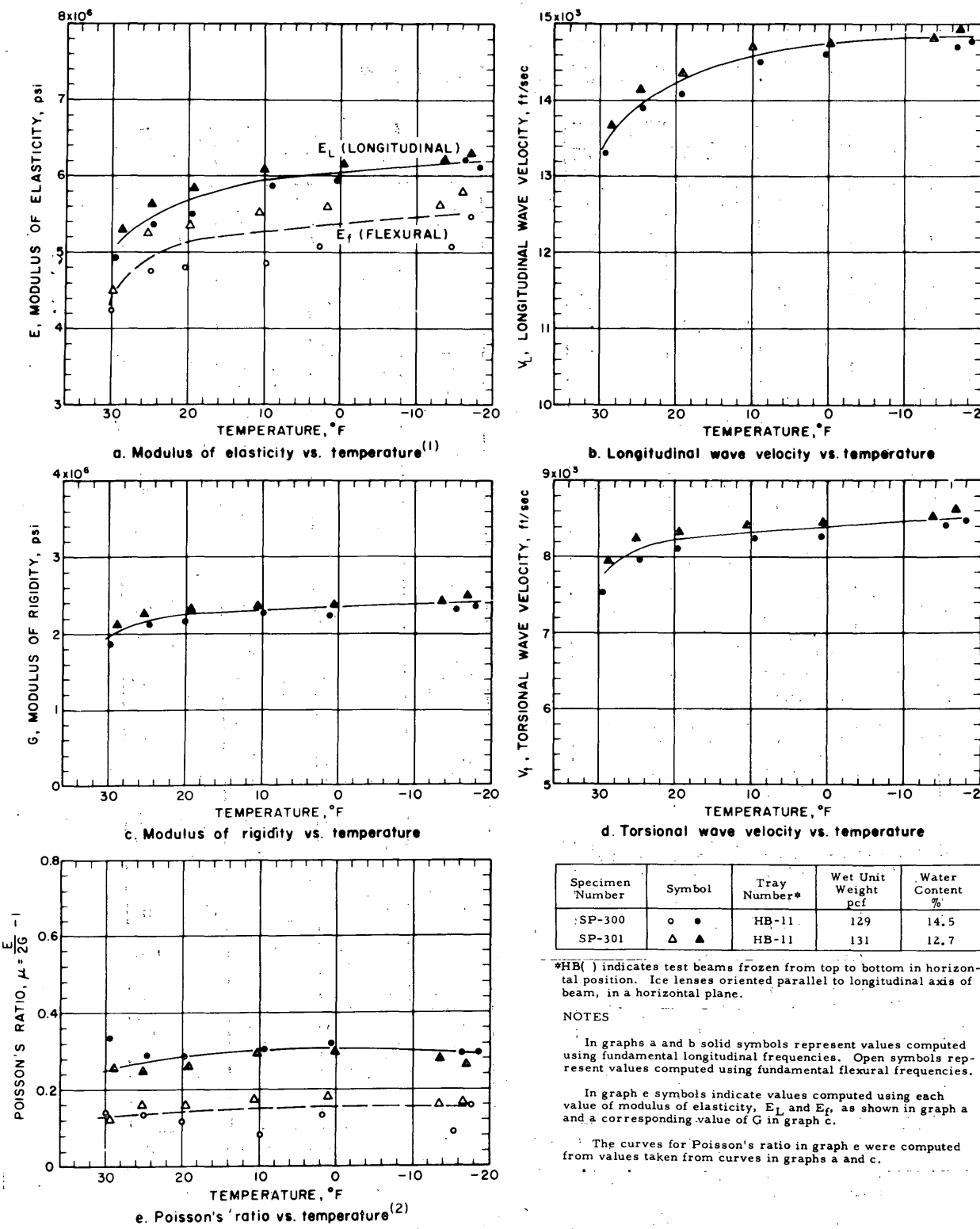

Specimen Number	Symbol	Tray Number*	Wet Unit Weight pcf	Water Content %
SP-300	○ ●	HB-11	129	14.5
SP-301	△ ▲	HB-11	131	12.7

*HB( ) indicates test beams frozen from top to bottom in horizontal position. Ice lenses oriented parallel to longitudinal axis of beam, in a horizontal plane.

NOTES

In graphs a and b solid symbols represent values computed using fundamental longitudinal frequencies. Open symbols represent values computed using fundamental flexural frequencies.

In graph e symbols indicate values computed using each value of modulus of elasticity, E_L and E_f, as shown in graph a and a corresponding value of G in graph c.

The curves for Poisson's ratio in graph e were computed from values taken from curves in graphs a and c.

Figure A1. Dynamic elastic properties of frozen Peabody gravelly sand vs temperature.

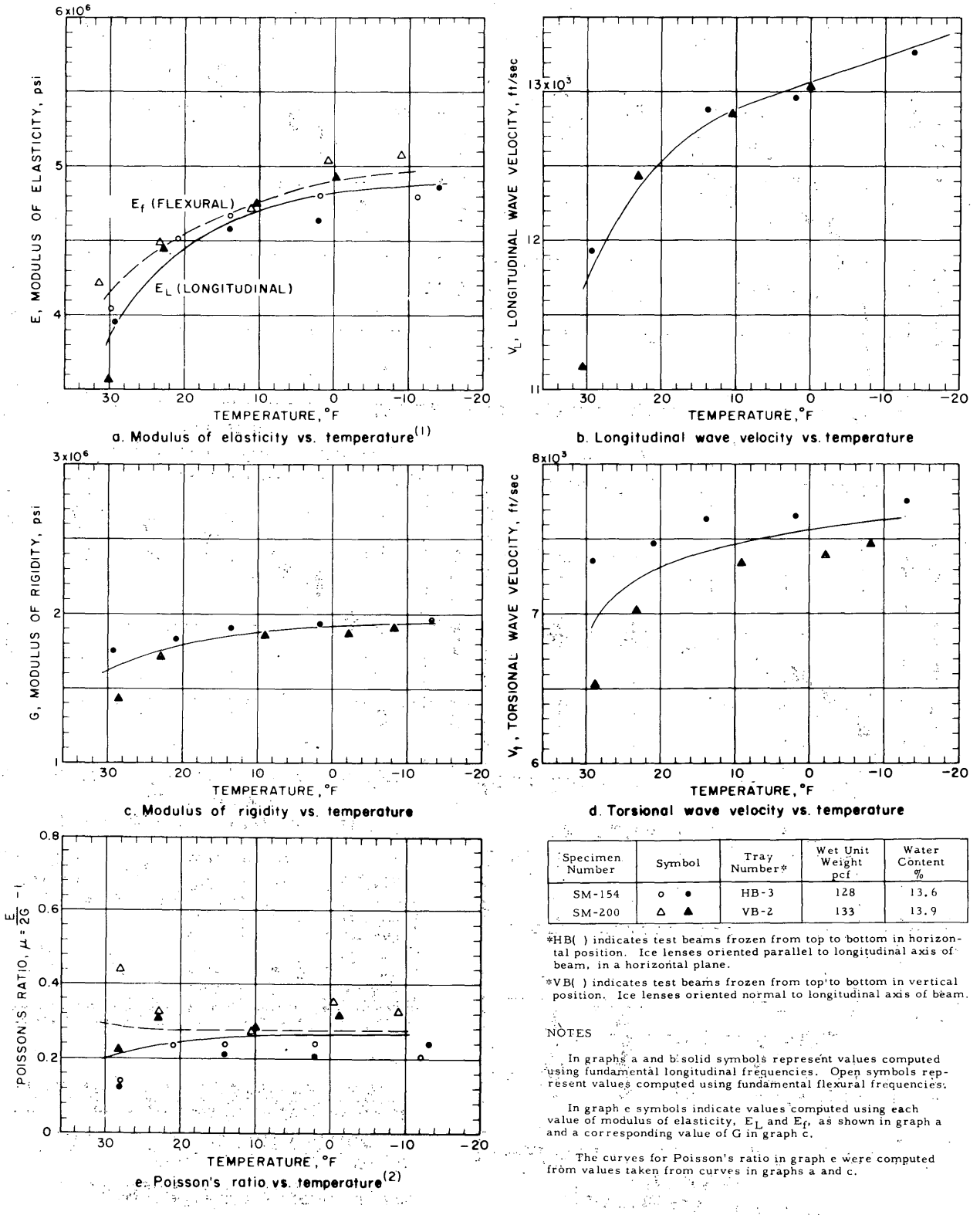

Specimen Number	Symbol	Tray Number*	Wet Unit Weight pcf	Water Content %
SM-154	○ ●	HB-3	128	13.6
SM-200	△ ▲	VB-2	133	13.9

*HB( ) indicates test beams frozen from top to bottom in horizontal position. Ice lenses oriented parallel to longitudinal axis of beam, in a horizontal plane.

*VB( ) indicates test beams frozen from top to bottom in vertical position. Ice lenses oriented normal to longitudinal axis of beam.

NOTES

In graphs a and b solid symbols represent values computed using fundamental longitudinal frequencies. Open symbols represent values computed using fundamental flexural frequencies.

In graph e symbols indicate values computed using each value of modulus of elasticity, E_L and E_f, as shown in graph a and a corresponding value of G in graph c.

The curves for Poisson's ratio in graph e were computed from values taken from curves in graphs a and c.

Figure A2. Dynamic elastic properties of frozen McNamara concrete sand vs temperature.

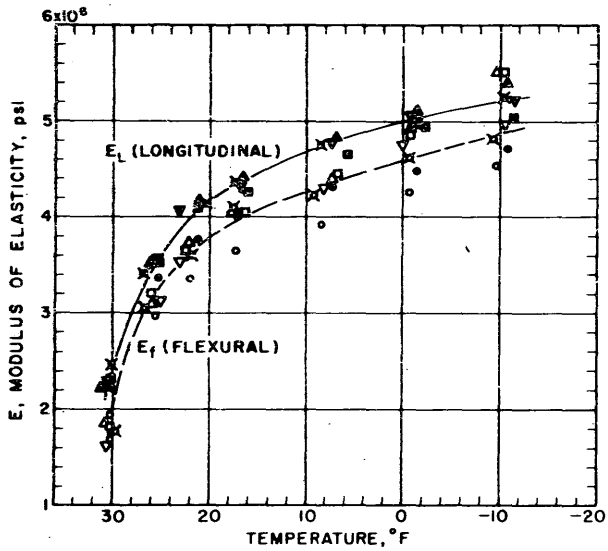

a. Modulus of elasticity vs. temperature[1]

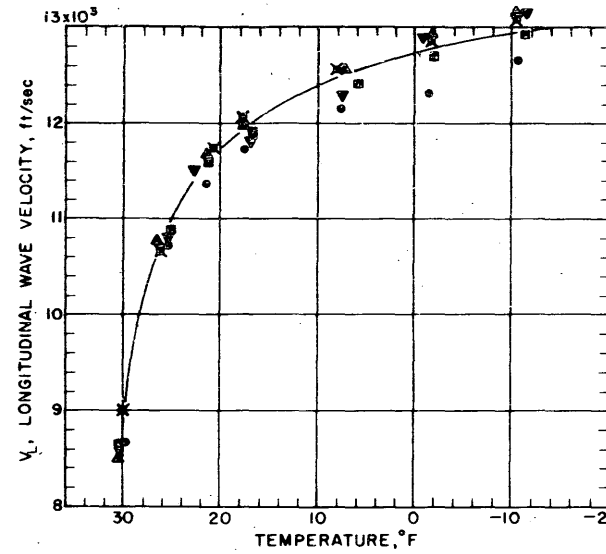

b. Longitudinal wave velocity vs. temperature

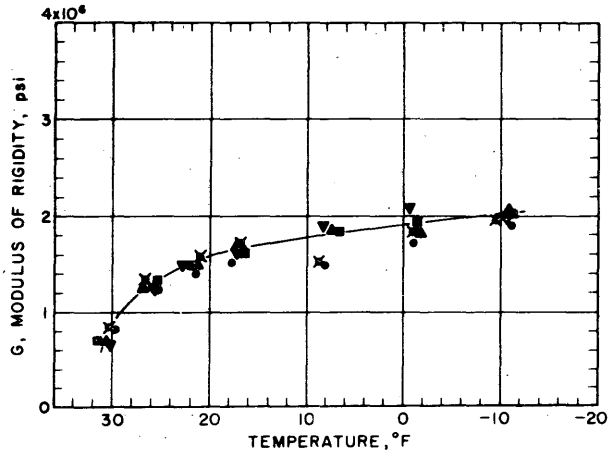

c. Modulus of rigidity vs. temperature

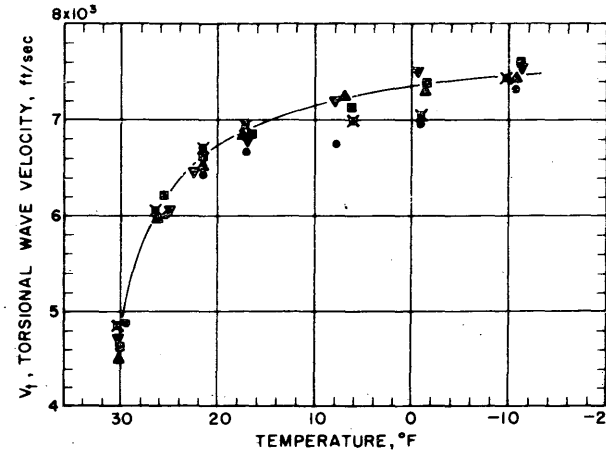

d. Torsional wave velocity vs. temperature

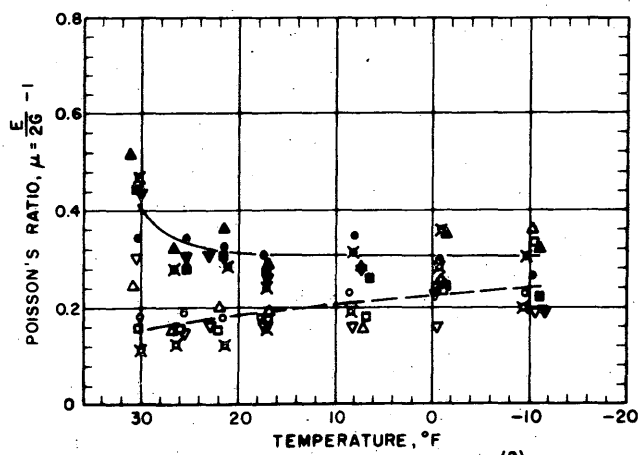

e. Poisson's ratio vs. temperature[2]

Specimen Number	Symbol	Tray Number*	Wet Unit Weight pcf	Water Content %
SMT-306	○ ●	VB-9	136	15.1
SMT-307	□ ■	VB-9	142	14.2
SMT-308	△ ▲	VB-9	143	12.5
SMT-309	▽ ▼	VB-9	142	12.2
SMT-310	⌘ ⌘	VB-9	139	12.1

*VB( ) indicates test beams frozen from top to bottom in vertical position. Ice lenses oriented normal to longitudinal axis of beam.

NOTES

In graphs a and b solid symbols represent values computed using fundamental longitudinal frequencies. Open symbols represent values computed using fundamental flexural frequencies.

In graph e symbols indicate values computed using each value of modulus of elasticity, E_L and E_f, as shown in graph a and a corresponding value of G in graph c.

The curves for Poisson's ratio in graph e were computed from values taken from curves in graphs a and c.

Figure A3. Dynamic elastic properties of frozen blend, McNamara concrete sand and East Boston till vs temperature.

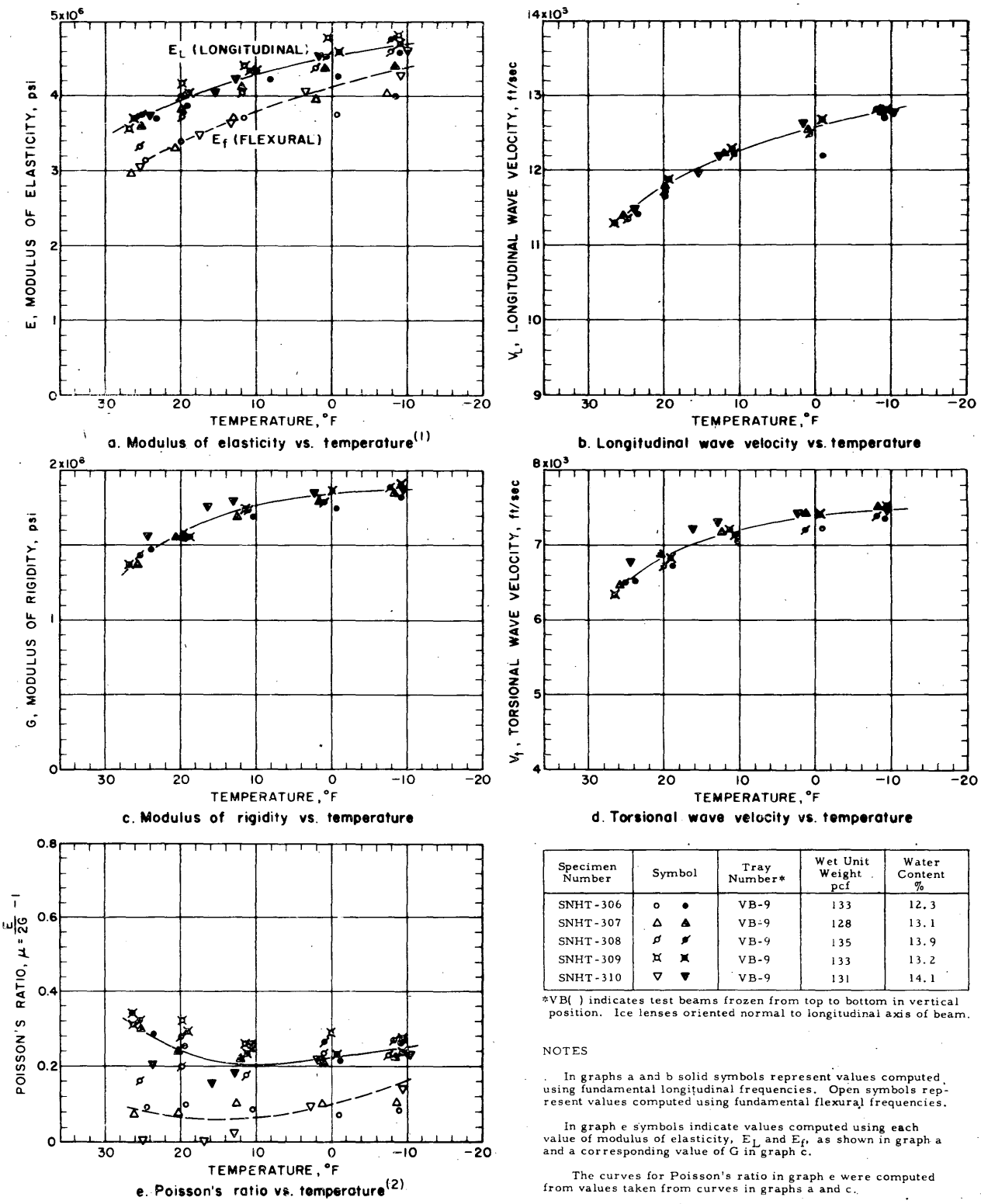

Specimen Number	Symbol	Tray Number*	Wet Unit Weight pcf	Water Content %
SNHT-306	○ ●	VB-9	133	12.3
SNHT-307	△ ▲	VB-9	128	13.1
SNHT-308	ø ø	VB-9	135	13.9
SNHT-309	⌘ ⌘	VB-9	133	13.2
SNHT-310	▽ ▼	VB-9	131	14.1

*VB( ) indicates test beams frozen from top to bottom in vertical position. Ice lenses oriented normal to longitudinal axis of beam.

NOTES

In graphs a and b solid symbols represent values computed using fundamental longitudinal frequencies. Open symbols represent values computed using fundamental flexural frequencies.

In graph e symbols indicate values computed using each value of modulus of elasticity, E_L and E_f, as shown in graph a and a corresponding value of G in graph c.

The curves for Poisson's ratio in graph e were computed from values taken from curves in graphs a and c.

Figure A4. Dynamic elastic properties of frozen blend, Manchester fine sand and East Boston till vs temperature.

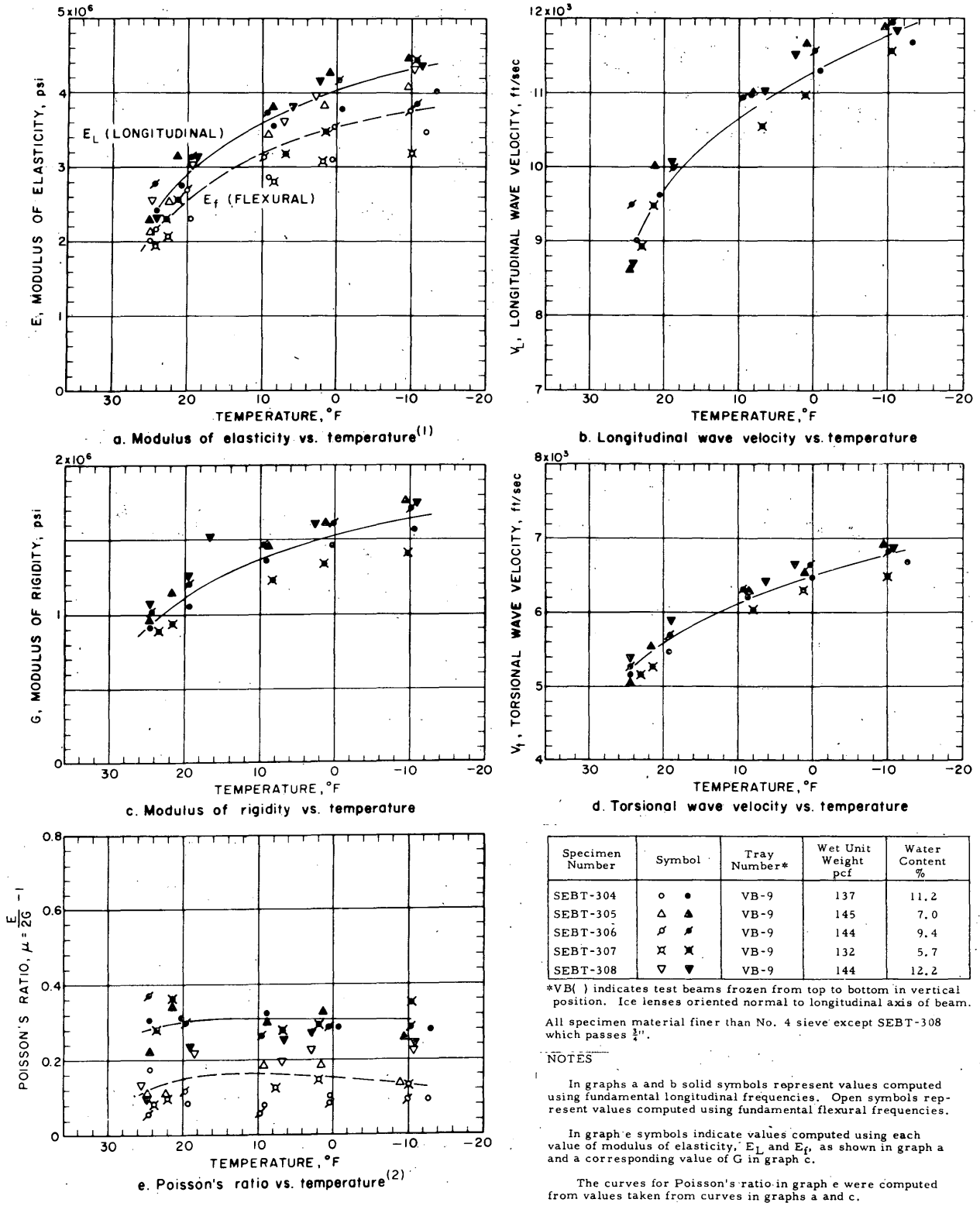

Specimen Number	Symbol	Tray Number*	Wet Unit Weight pcf	Water Content %
SEBT-304	○ ●	VB-9	137	11.2
SEBT-305	△ ▲	VB-9	145	7.0
SEBT-306	ø ø	VB-9	144	9.4
SEBT-307	⌘ ⌘	VB-9	132	5.7
SEBT-308	▽ ▼	VB-9	144	12.2

*VB( ) indicates test beams frozen from top to bottom in vertical position. Ice lenses oriented normal to longitudinal axis of beam.

All specimen material finer than No. 4 sieve except SEBT-308 which passes ¾".

NOTES

In graphs a and b solid symbols represent values computed using fundamental longitudinal frequencies. Open symbols represent values computed using fundamental flexural frequencies.

In graph e symbols indicate values computed using each value of modulus of elasticity, E_L and E_f, as shown in graph a and a corresponding value of G in graph c.

The curves for Poisson's ratio in graph e were computed from values taken from curves in graphs a and c.

Figure A5. Dynamic elastic properties of frozen East Boston till vs temperature.

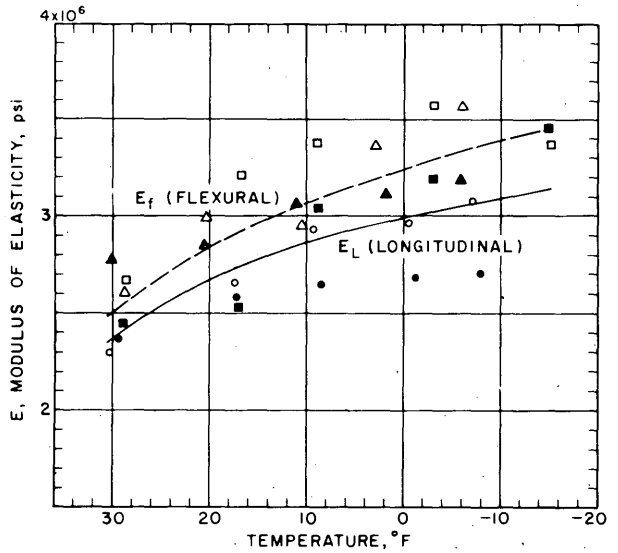

a. Modulus of elasticity vs. temperature[1]

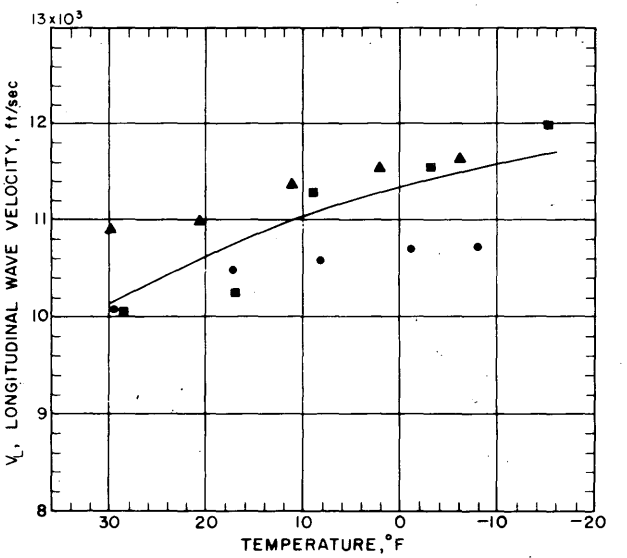

b. Longitudinal wave velocity vs. temperature

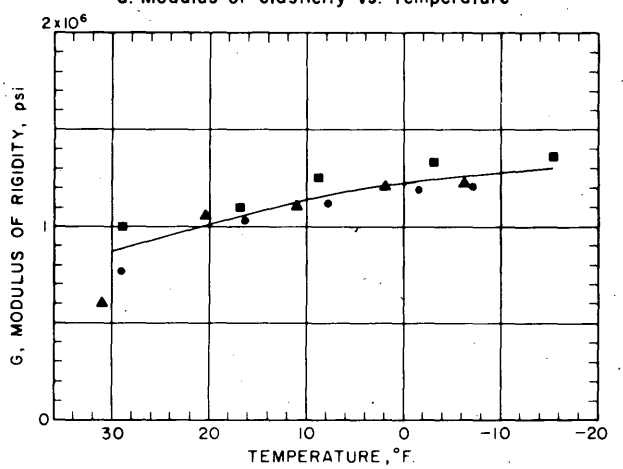

c. Modulus of rigidity vs. temperature

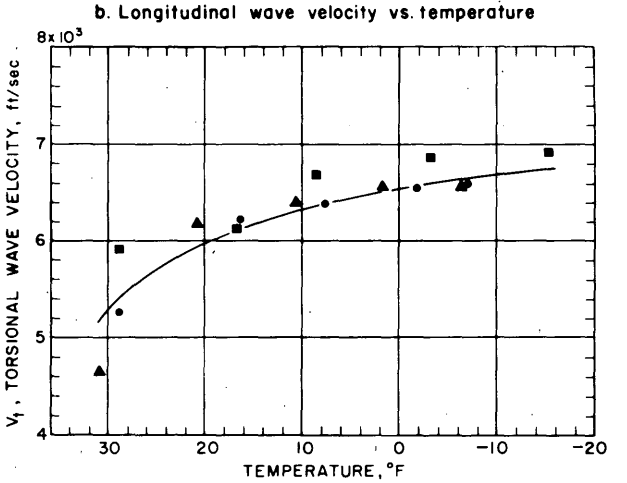

d. Torsional wave velocity vs. temperature

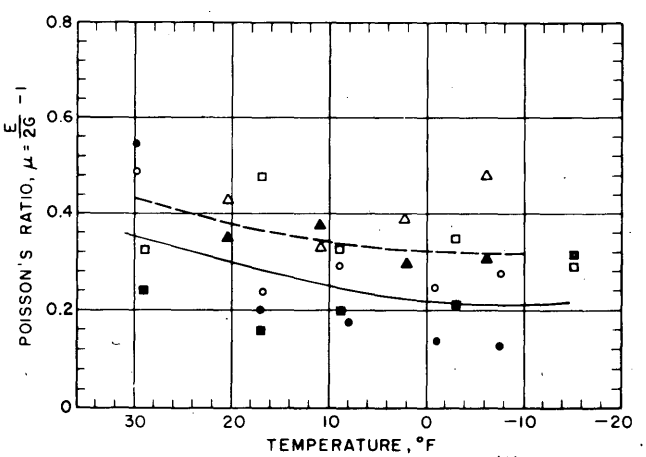

e. Poisson's ratio vs. temperature[2]

Specimen Number	Symbol	Tray Number*	Wet Unit Weight pcf	Water Content %
SNHS-150	○ ●	VB-2	109	41.5
SNHS-152	△ ▲	HB-3	109	28.1
SNHS-153	□ ■	HB-3	112	31.4

*HB( ) indicates test beams frozen from top to bottom in horizontal position. Ice lenses oriented parallel to longitudinal axis of beam, in a horizontal plane.

*VB( ) indicates test beams frozen from top to bottom in vertical position. Ice lenses oriented normal to longitudinal axis of beam.

NOTES

In graphs a and b solid symbols represent values computed using fundamental longitudinal frequencies. Open symbols represent values computed using fundamental flexural frequencies.

In graph e symbols indicate values computed using each value of modulus of elasticity, E_L and E_f, as shown in graph a and a corresponding value of G in graph c.

The curves for Poisson's ratio in graph e were computed from values taken from curves in graphs a and c.

Figure A6. Dynamic elastic properties of frozen New Hampshire silt vs temperature.

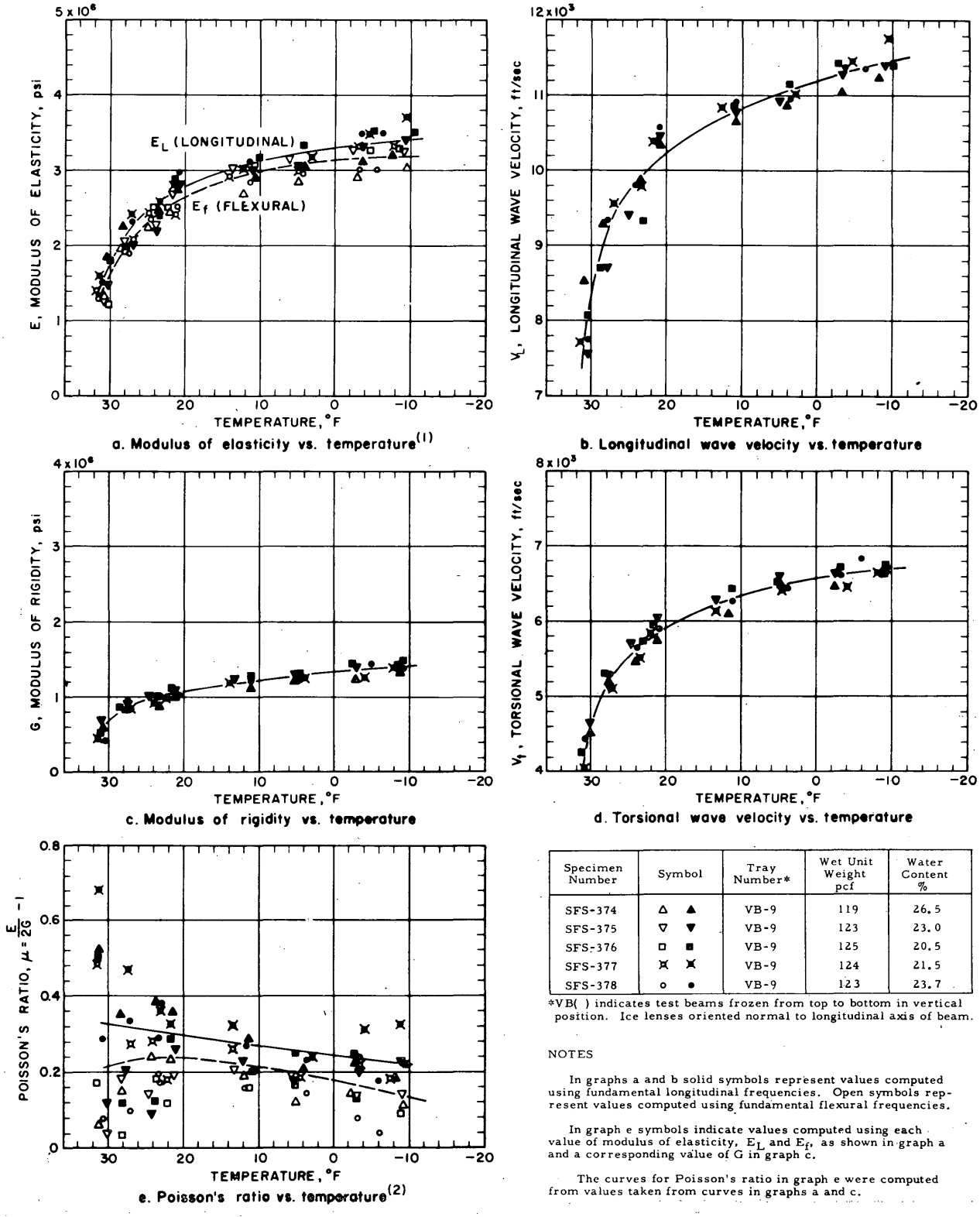

Specimen Number	Symbol	Tray Number*	Wet Unit Weight pcf	Water Content %
SFS-374	△ ▲	VB-9	119	26.5
SFS-375	▽ ▼	VB-9	123	23.0
SFS-376	□ ■	VB-9	125	20.5
SFS-377	⌘ ⌘	VB-9	124	21.5
SFS-378	○ ●	VB-9	123	23.7

*VB( ) indicates test beams frozen from top to bottom in vertical position. Ice lenses oriented normal to longitudinal axis of beam.

NOTES

In graphs a and b solid symbols represent values computed using fundamental longitudinal frequencies. Open symbols represent values computed using fundamental flexural frequencies.

In graph e symbols indicate values computed using each value of modulus of elasticity, E_L and E_f, as shown in graph a and a corresponding value of G in graph c.

The curves for Poisson's ratio in graph e were computed from values taken from curves in graphs a and c.

Figure A7. Dynamic elastic properties of frozen Fairbanks silt vs temperature.

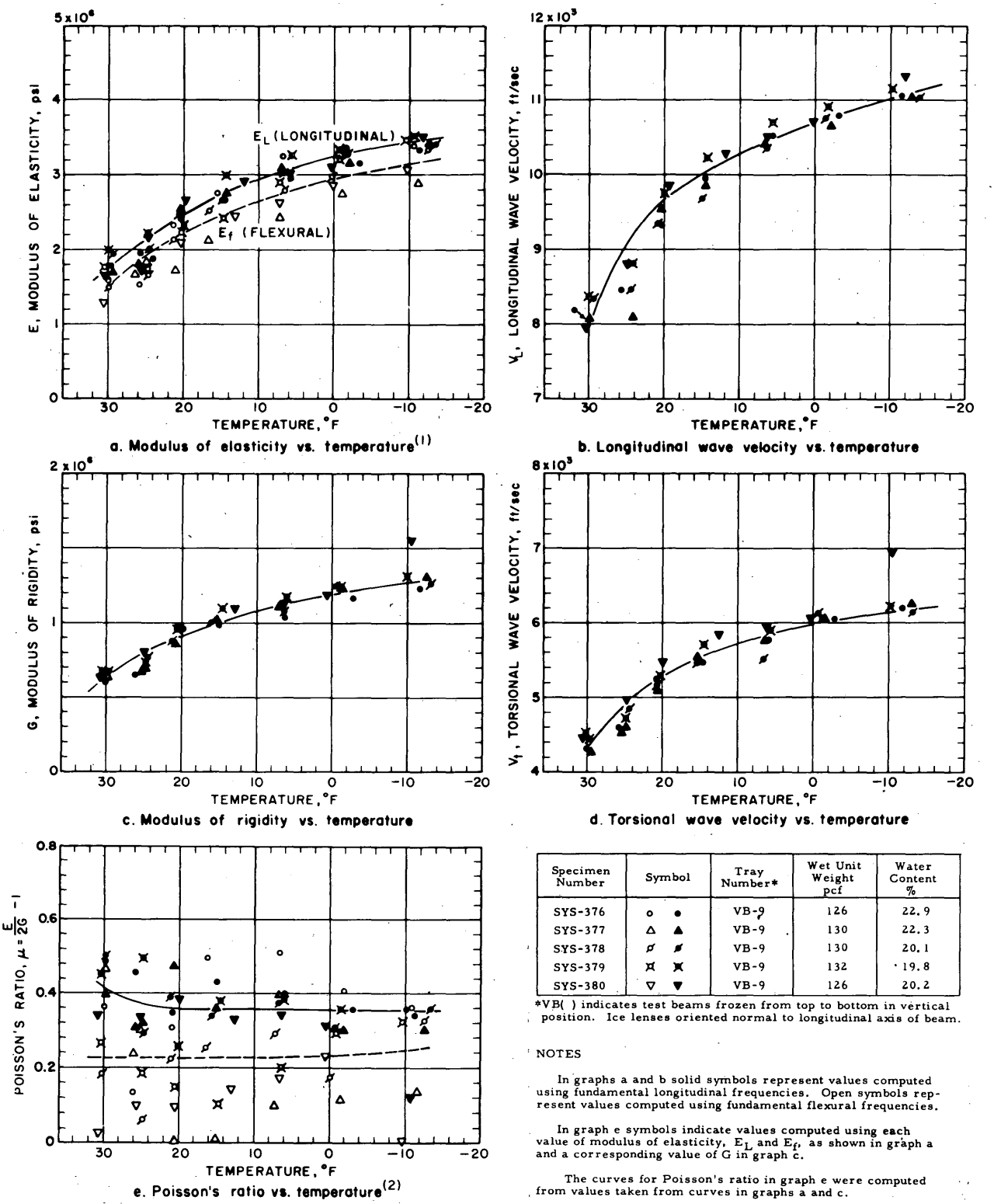

Specimen Number	Symbol	Tray Number*	Wet Unit Weight pcf	Water Content %
SYS-376	○ ●	VB-9	126	22.9
SYS-377	△ ▲	VB-9	130	22.3
SYS-378	ø ø	VB-9	130	20.1
SYS-379	⌘ ⌘	VB-9	132	19.8
SYS-380	▽ ▼	VB-9	126	20.2

*VB( ) indicates test beams frozen from top to bottom in vertical position. Ice lenses oriented normal to longitudinal axis of beam.

NOTES

In graphs a and b solid symbols represent values computed using fundamental longitudinal frequencies. Open symbols represent values computed using fundamental flexural frequencies.

In graph e symbols indicate values computed using each value of modulus of elasticity, E_L and E_f, as shown in graph a and a corresponding value of G in graph c.

The curves for Poisson's ratio in graph e were computed from values taken from curves in graphs a and c.

Figure A8. Dynamic elastic properties of frozen Yukon silt vs temperature.

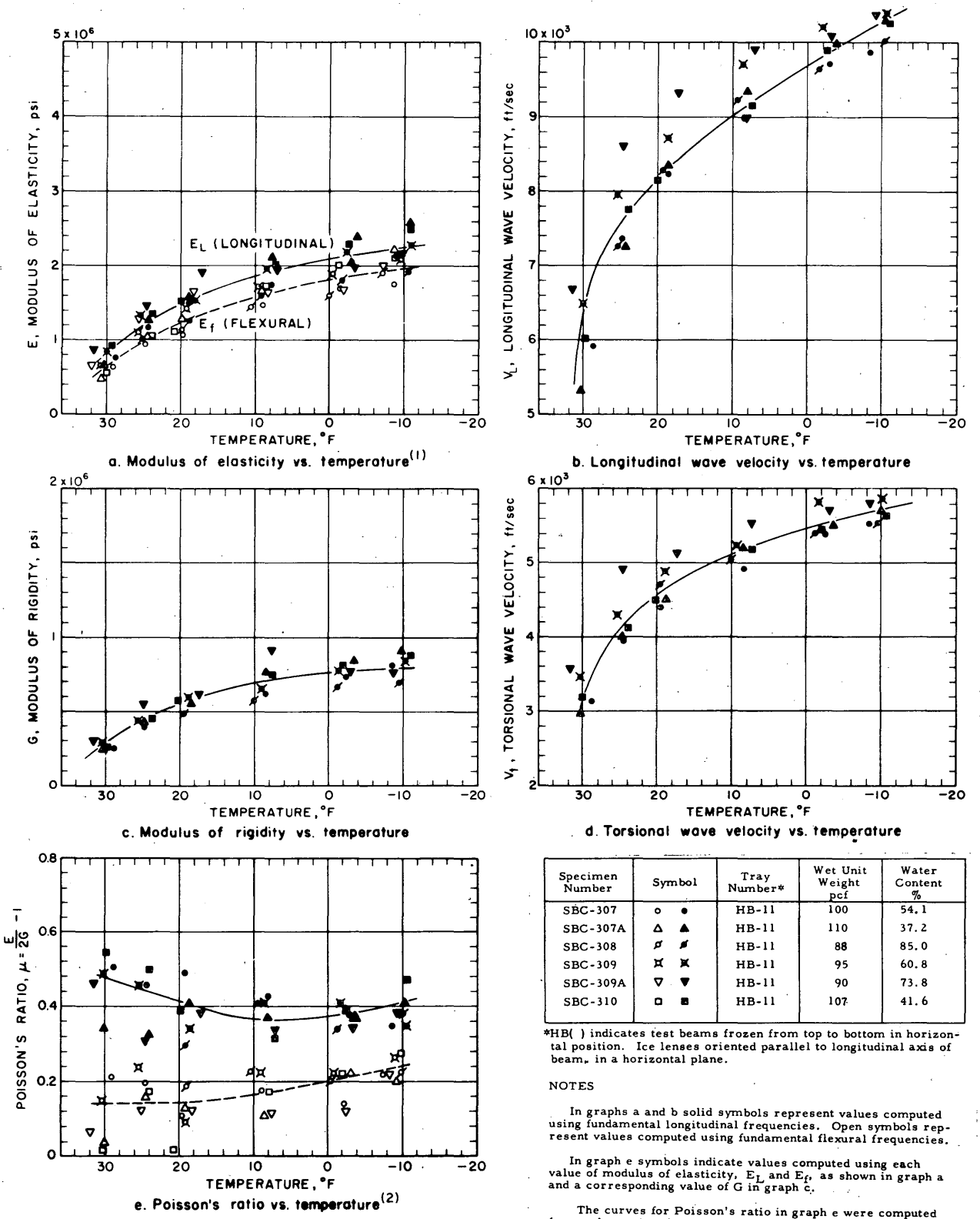

Specimen Number	Symbol	Tray Number*	Wet Unit Weight pcf	Water Content %
SBC-307	○ ●	HB-11	100	54.1
SBC-307A	△ ▲	HB-11	110	37.2
SBC-308	⌀ ⌀	HB-11	88	85.0
SBC-309	✕ ✕	HB-11	95	60.8
SBC-309A	▽ ▼	HB-11	90	73.8
SBC-310	□ ■	HB-11	107	41.6

*HB( ) indicates test beams frozen from top to bottom in horizontal position. Ice lenses oriented parallel to longitudinal axis of beam, in a horizontal plane.

NOTES

In graphs a and b solid symbols represent values computed using fundamental longitudinal frequencies. Open symbols represent values computed using fundamental flexural frequencies.

In graph e symbols indicate values computed using each value of modulus of elasticity, E_L and E_f, as shown in graph a and a corresponding value of G in graph c.

The curves for Poisson's ratio in graph e were computed from values taken from curves in graphs a and c.

Figure A9. Dynamic elastic properties of frozen Boston blue clay vs temperature.

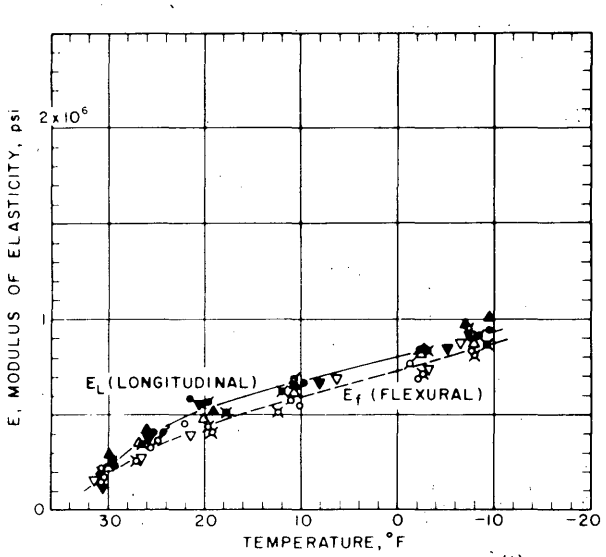

a. Modulus of elasticity vs. temperature[1]

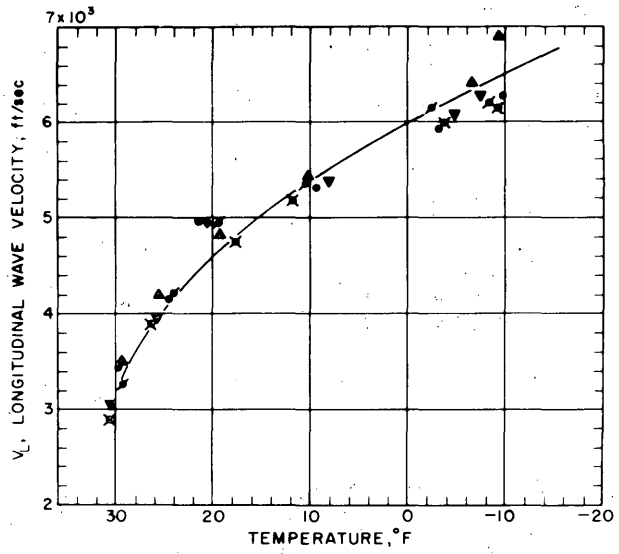

b. Longitudinal wave velocity vs. temperature

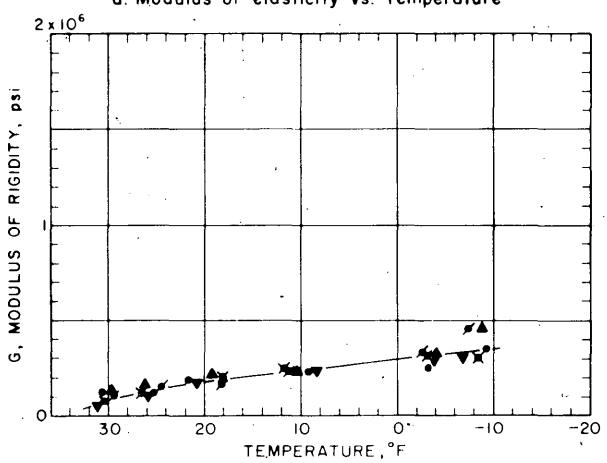

c. Modulus of rigidity vs. temperature

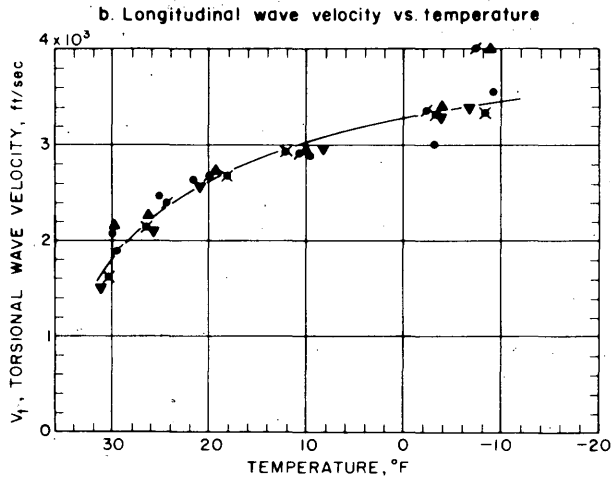

d. Torsional wave velocity vs. temperature

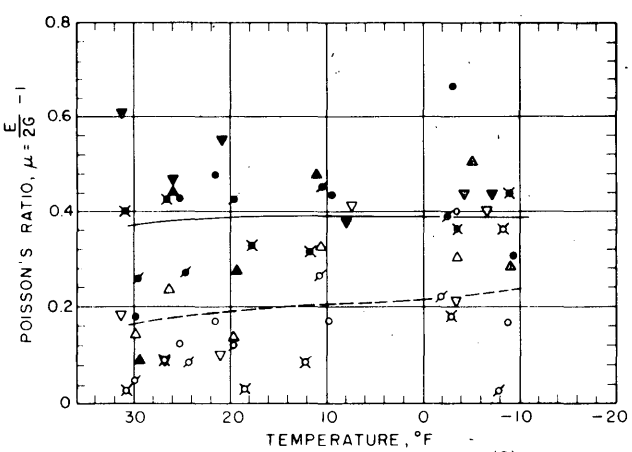

e. Poisson's ratio vs. temperature[2]

Specimen Number	Symbol	Tray Number*	Wet Unit Weight pcf	Water Content %
SFFC-366	○ ●	HB-11	111	33.5
SFFC-366A	△ ▲	HB-11	108	33.4
SFFC-367	ø ø	HB-11	109	35.6
SFFC-368	⌑ ⌑	HB-11	108	34.5
SFFC-369	▽ ▼	HB-11	108	35.3

*HB( ) indicates test beams frozen from top to bottom in horizontal position. Ice lenses oriented parallel to longitudinal axis of beam, in a horizontal plane.

NOTES

In graphs a and b solid symbols represent values computed using fundamental longitudinal frequencies. Open symbols represent values computed using fundamental flexural frequencies.

In graph e symbols indicate values computed using each value of modulus of elasticity, E_L and E_f, as shown in graph a and a corresponding value of G in graph c.

The curves for Poisson's ratio in graph e were computed from values taken from curves in graphs a and c.

Figure A10. Dynamic elastic properties of frozen Fargo clay vs temperature.

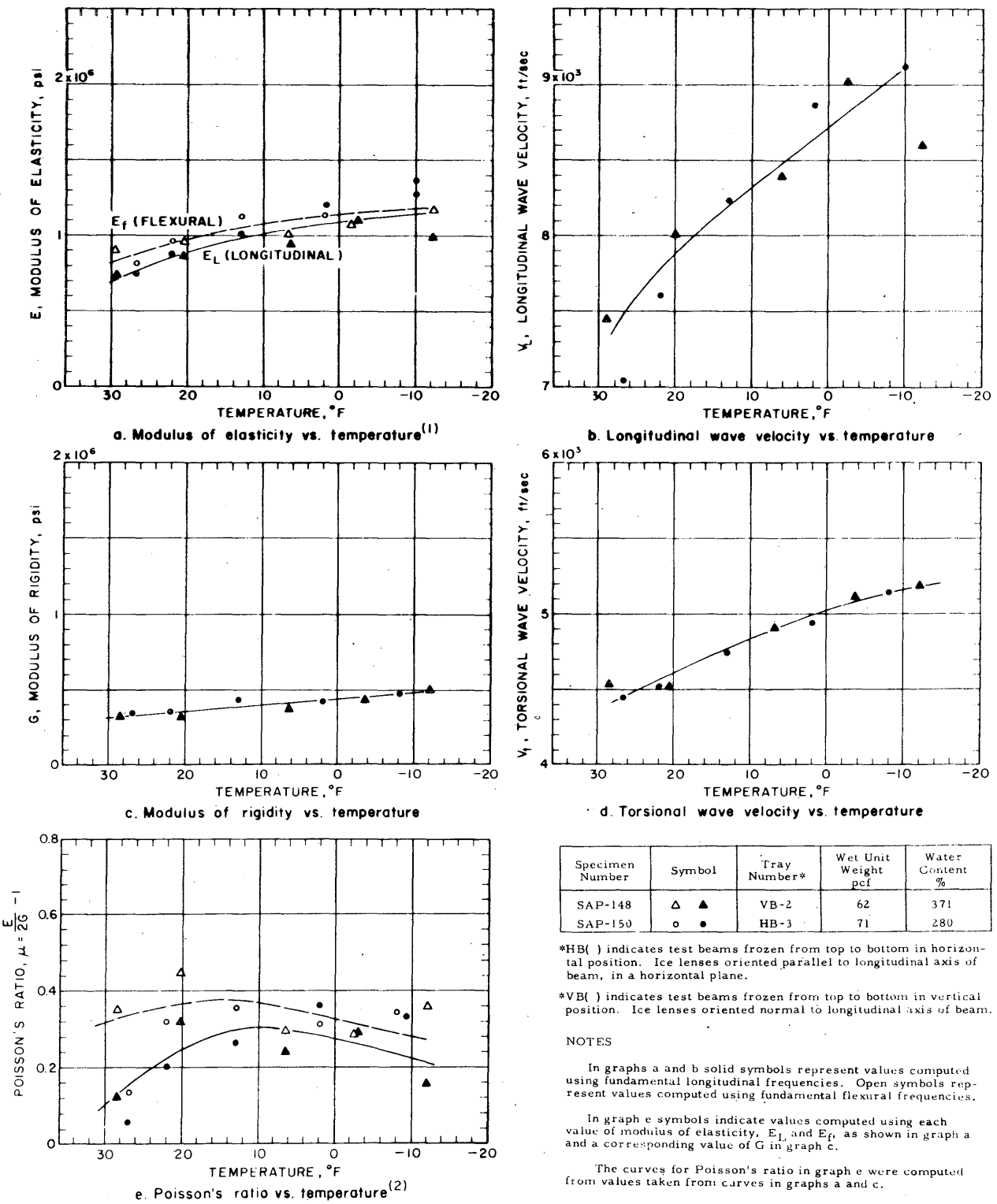

Specimen Number	Symbol	Tray Number*	Wet Unit Weight pcf	Water Content %
SAP-148	△ ▲	VB-2	62	371
SAP-150	○ ●	HB-3	71	280

*HB( ) indicates test beams frozen from top to bottom in horizontal position. Ice lenses oriented parallel to longitudinal axis of beam, in a horizontal plane.

*VB( ) indicates test beams frozen from top to bottom in vertical position. Ice lenses oriented normal to longitudinal axis of beam.

NOTES

In graphs a and b solid symbols represent values computed using fundamental longitudinal frequencies. Open symbols represent values computed using fundamental flexural frequencies.

In graph e symbols indicate values computed using each value of modulus of elasticity, E_L and E_f, as shown in graph a and a corresponding value of G in graph c.

The curves for Poisson's ratio in graph e were computed from values taken from curves in graphs a and c.

Figure A11. Dynamic elastic properties of frozen Alaska peat vs temperature.

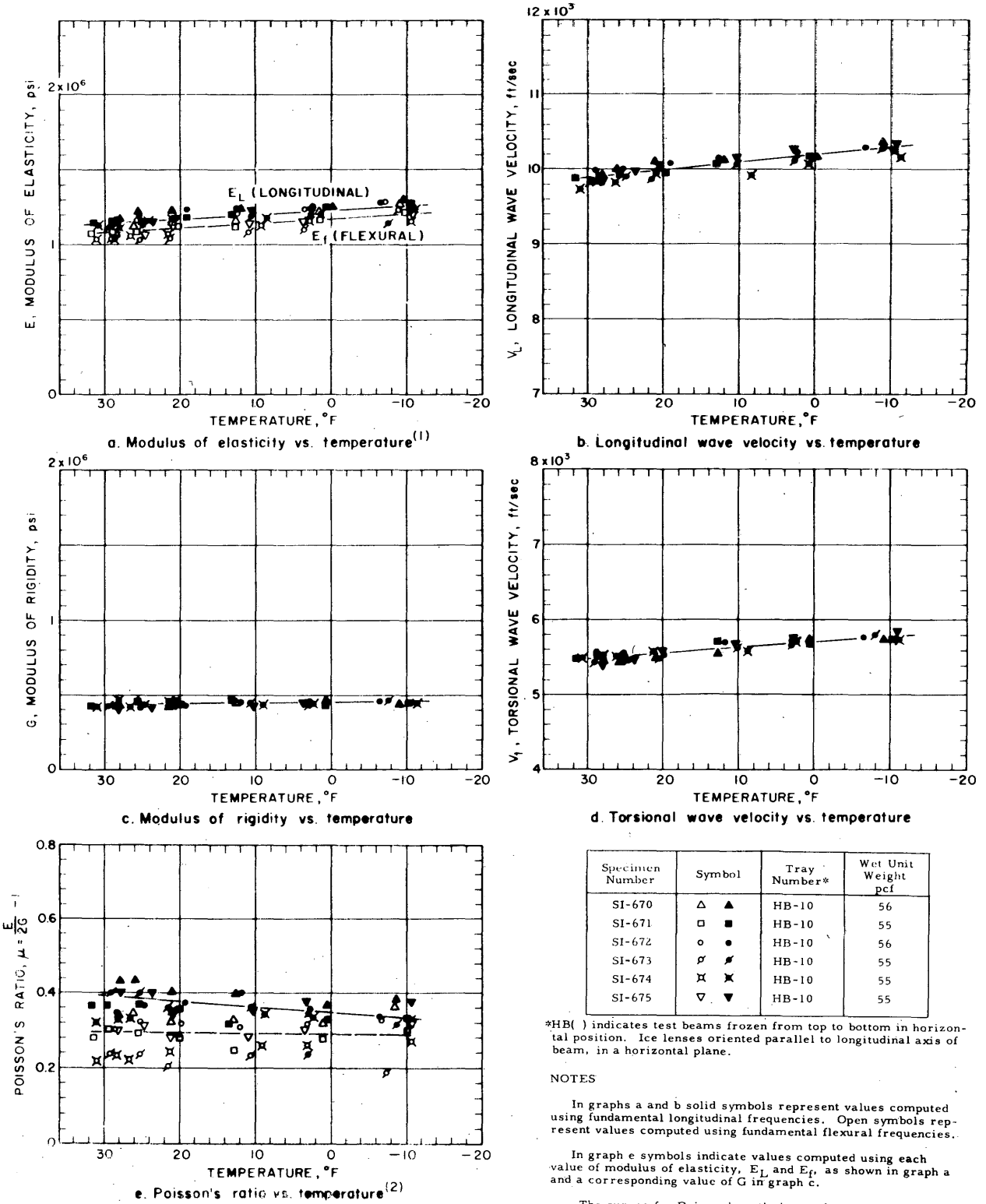

Specimen Number	Symbol	Tray Number*	Wet Unit Weight pcf
SI-670	△ ▲	HB-10	56
SI-671	□ ■	HB-10	55
SI-672	○ ●	HB-10	56
SI-673	⌀ ⌀	HB-10	55
SI-674	⌘ ⌘	HB-10	55
SI-675	▽ ▼	HB-10	55

*HB( ) indicates test beams frozen from top to bottom in horizontal position. Ice lenses oriented parallel to longitudinal axis of beam, in a horizontal plane.

NOTES

In graphs a and b solid symbols represent values computed using fundamental longitudinal frequencies. Open symbols represent values computed using fundamental flexural frequencies.

In graph e symbols indicate values computed using each value of modulus of elasticity, E_L and E_f, as shown in graph a and a corresponding value of G in graph c.

The curves for Poisson's ratio in graph e were computed from values taken from curves in graphs a and c.

Figure A12. Dynamic elastic properties of artificially frozen ice (tray HB-10) vs temperature.

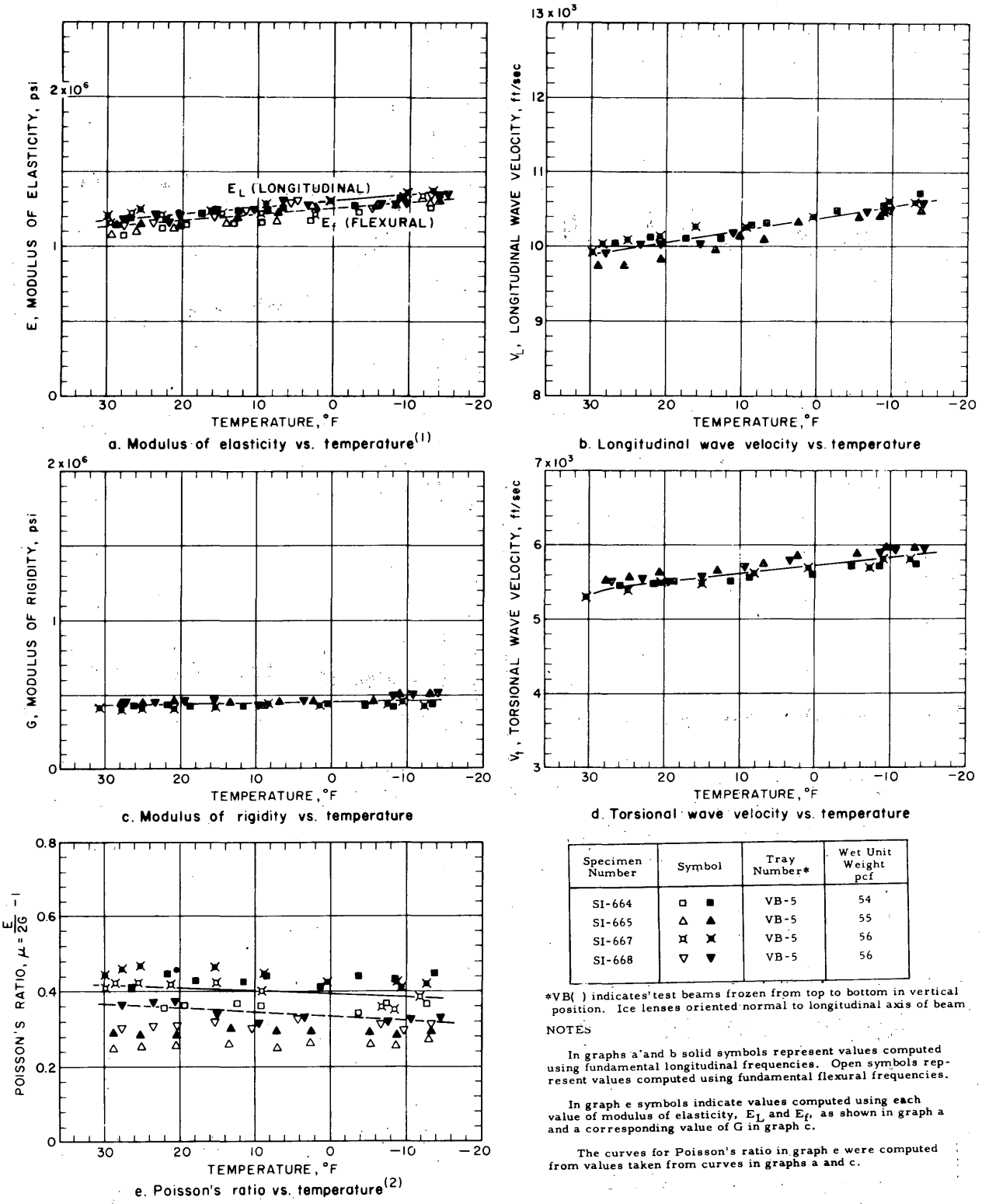

Specimen Number	Symbol	Tray Number*	Wet Unit Weight pcf
SI-664	□ ■	VB-5	54
SI-665	△ ▲	VB-5	55
SI-667	⌘ ⌘	VB-5	56
SI-668	▽ ▼	VB-5	56

*VB( ) indicates test beams frozen from top to bottom in vertical position. Ice lenses oriented normal to longitudinal axis of beam

NOTES

In graphs a and b solid symbols represent values computed using fundamental longitudinal frequencies. Open symbols represent values computed using fundamental flexural frequencies.

In graph e symbols indicate values computed using each value of modulus of elasticity, E_L and E_f, as shown in graph a and a corresponding value of G in graph c.

The curves for Poisson's ratio in graph e were computed from values taken from curves in graphs a and c.

Figure A13. Dynamic elastic properties of artificially frozen ice (tray VB-5) vs temperature.

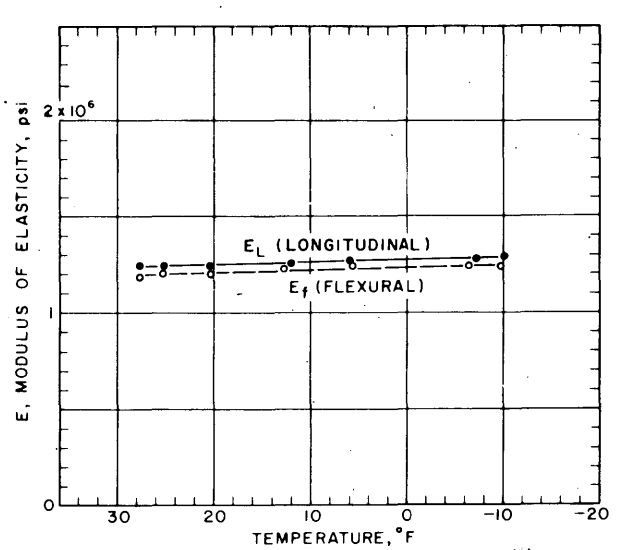

a. Modulus of elasticity vs. temperature[1]

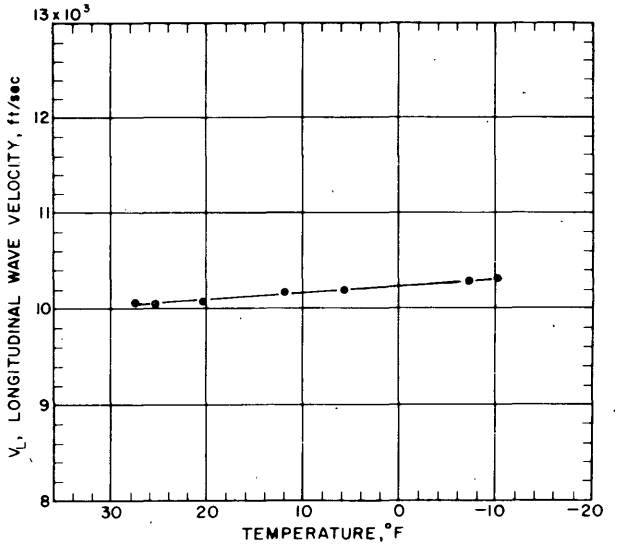

b. Longitudinal wave velocity vs. temperature

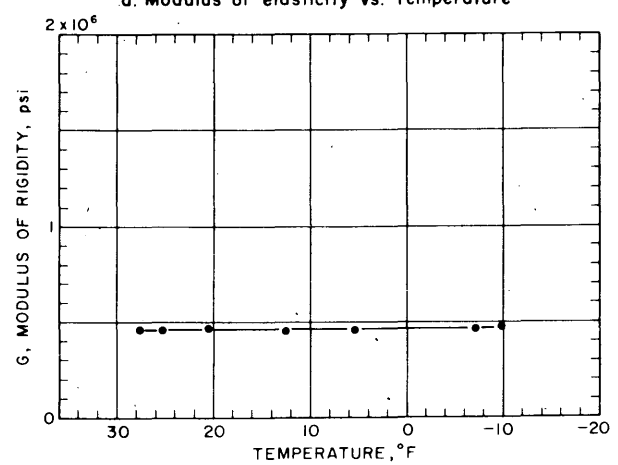

c. Modulus of rigidity vs. temperature

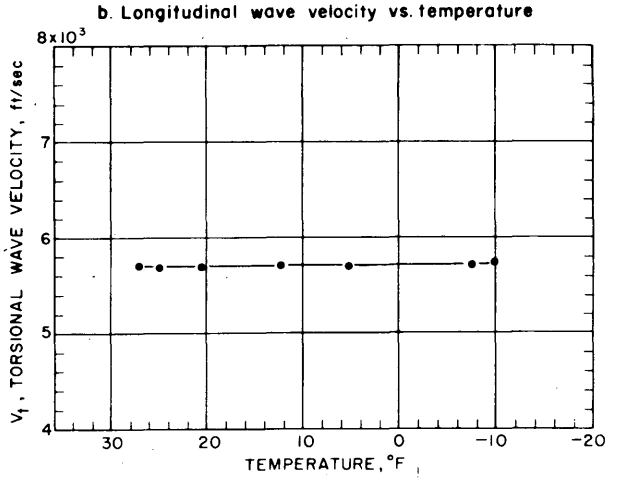

d. Torsional wave velocity vs. temperature

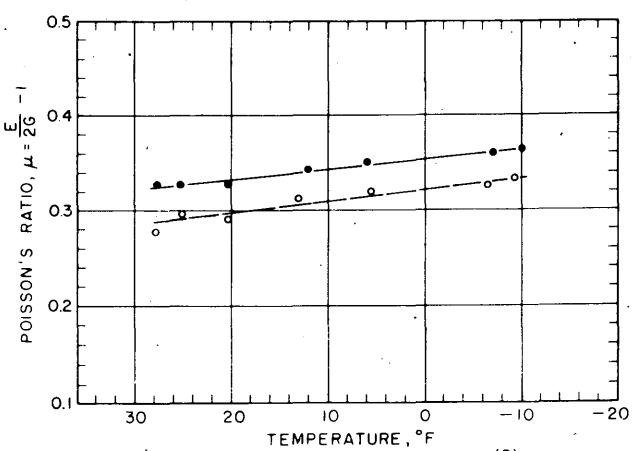

e. Poisson's ratio vs. temperature[2]

Specimen No.	Ice Type	Length, in.	Cross-sectional area, sq in.	Weight, lb	Density, lb/cu. in.
SI-(P)	Clear	9.95	2.24	0.725	0.0326

Horizontal Beam (Optic Axes of crystals oriented normal to longitudinal axis of beam.)

NOTES

In graphs a and b solid symbols represent values computed using fundamental longitudinal frequencies. Open symbols represent values computed using fundamental flexural frequencies.

In graph e symbols indicate values computed using each value of modulus of elasticity, E_L and E_f, as shown in graph a and a corresponding value of G in graph c.

The curves for Poisson's ratio in graph e were computed from values taken from curves in graphs a and c.

Figure A14. Dynamic elastic properties of Portage Lake (natural) ice vs temperature.

Unclassified

Security Classification

DOCUMENT CONTROL DATA - R & D

(Security classification of title, body of abstract and indexing annotation must be entered when the overall report is classified)

1. ORIGINATING ACTIVITY *(Corporate author)*

Cold Regions Research & Engineering Laboratory
U.S. Army Terrestrial Sciences Center
Hanover, New Hampshire

2a. REPORT SECURITY CLASSIFICATION

Unclassified

2b. GROUP

3. REPORT TITLE

LABORATORY DETERMINATION OF THE DYNAMIC MODULI OF FROZEN SOILS AND OF ICE

4. DESCRIPTIVE NOTES *(Type of report and inclusive dates)*

Research Report

5. AUTHOR(S) *(First name, middle initial, last name)*

Chester W. Kaplar

6. REPORT DATE

January 1969

7a. TOTAL NO. OF PAGES

48

7b. NO. OF REFS

73

8a. CONTRACT OR GRANT NO.

b. PROJECT NO.

c. DA Task 1T062112A13001

d.

9a. ORIGINATOR'S REPORT NUMBER(S)

Research Report 163

9b. OTHER REPORT NO(S) *(Any other numbers that may be assigned this report)*

10. DISTRIBUTION STATEMENT

This document has been approved for public release and sale; its distribution is unlimited

11. SUPPLEMENTARY NOTES

Co-sponsored by
Office, Chief of Engineers
Directorate of Military Construction
Engineering Division
Civil Engineering Branch

12. SPONSORING MILITARY ACTIVITY

Cold Regions Research and Engineering Laboratory
U.S. Army Terrestrial Sciences Center
Hanover, New Hampshire

13. ABSTRACT

This report presents a summary of results of laboratory investigations of frozen soils and ice to determine the elastic moduli by the dynamic (sonic) method. The elastic moduli were indirectly obtained by measuring the fundamental resonant frequencies of flexural, longitudinal, and torsional vibrations induced in prismatic beams by electromagnetic means. Vibration tests were performed on a total of 56 specimens representing 12 different materials (8 natural soil types, ranging from coarse-grained to fine-grained; 2 blended soils; a natural peat; laboratory-frozen ice and natural lake ice, at temperatures ranging from approximately +32F to -10F). Elastic wave velocities (longitudinal and torsional) were computed for each material in the range of test temperatures studied. All soils were saturated or were close to saturation. The dynamic moduli of elasticity of the frozen soils were found to increase with a decrease in temperature, the greatest rate of increase occurring between +32F and +20F. Coarse granular soils gave the highest values and clays the lowest in the ratio of more than 4 to 1. Dynamic Young's modulus, E, computed from flexural vibrations was usually lower than dynamic E computed from longitudinal vibrations. Average values of dynamic Poisson's ratio for all soil types computed from average values of E and G (longitudinal vibrations) ranged from 0.26 to 0.38. Values of Poisson's ratio for the various soil types did not conform to any logical pattern related to temperature or soil type. The dynamic moduli of elasticity of ice showed only slight dependence on temperature, and test values were more consistent than those of the soils. Natural lake ice was

(Cont'd)

DD FORM 1 NOV 65 1473 REPLACES DD FORM 1473, 1 JAN 64, WHICH IS OBSOLETE FOR ARMY USE.

Unclassified

Security Classification

14. KEY WORDS	LINK A ROLE	LINK A WT	LINK B ROLE	LINK B WT	LINK C ROLE	LINK C WT
Frozen soil Ice Dynamic moduli of elasticity Vibration Elastic wave velocity Young's modulus Poisson's ratio						

Abstract (Cont'd)

least temperature dependent and gave the most consistent results. Dynamic moduli of ice E (longitudinal vibration) and G compared closely with values reported by other investigators. Average values of Poisson's ratio for ice were reasonable but less consistent, ranging from 0.30 to 0.41.